Final Draft
of the original manuscript:

Ungar, G.; Tschierske, C.; Abetz, V.; Holyst, R.; Bates, M.A.; Lui, F.; Prehm, M.; Kieffer, R.; Zeng, X.; Walker, M.; Glettner, B.; Zywocinski, A.:

Self-Assembly at Different Length Scales: Polyphilic Star-Branched Liquid Crystals and Miktoarm Star Copolymers

In: Advanced Functional Materials (2011) Wiley

DOI: 10.1002/adfm.201002091

Self-Assembly at Different Length Scales: Polyphilic Star-Branched Liquid Crystals and Mictoarm Star Copolymers

By *G. Ungar*,* *C. Tschierske*,* *V. Abetz*, *R. Holyst*, *M. A. Bates*, *F. Liu*, *M. Prehm*, *R. Kieffer*, *X B. Zeng*, *M. Walker*, *B. Glettner*, *A. Zywocinski*

[*] Prof. G. Ungar, Dr. X. B. Zeng, Dr. F. Liu
Department of Materials Science and Engineering, University of Sheffield, Mappin St., Sheffield S1 3JD (U.K.)
E-mail: g.ungar@shef.ac.uk
[*] Prof. Dr. C. Tschierske, Dr. M. Prehm, Dr. R. Kieffer, Dr. B. Glettner
Organic Chemistry, Institute of Chemistry, Martin-Luther-University Halle-Wittenberg, Kurt-Mothes-Str. 2, D-06120 Halle (Germany)
E-mail: carsten.tschierske@chemie.uni-halle.de
Prof. Dr. V. Abetz
Helmholtz-Zentrum Geesthacht, Institute of Polymer Research, Max-Planck-Str. 1, 21502 Geesthacht (Germany)
Prof. Dr. R. Holyst, Dr. A. Zywocinski
Institute of Physical Chemistry, Polish Academy of Science, Kasprzaka 44/52, 01-224 Warsaw (Poland)
Dr. M. A. Bates, Dr. M. Walker
Department of Chemistry, University of York, York, YO10 5DD (U.K.)

Keywords: columnar liquid crystals, polygonal honeycombs, polyphiles, miktoarm star terpolymers, simulation, Langmuir films, rod-coil molecules, surface alignment

Abstract: This article reviews the diversity of phase morphologies observed recently in star-branched liquid crystalline and polymeric compounds containing at least three immiscible segments. Bolaamphiphiles and facial amphiphiles with a rod-like aromatic core, two end-groups and one (T-shape) or two chains (X-shape) attached laterally to the core form numerous honeycomb-like liquid crystal phases, as well as a variety of novel lamellar and 3D-ordered mesophases. Molecular self-organization is described in bulk phases and in thin films on solid and liquid surfaces, as well as in Langmuir-Blodgett films. The remarkably reversible formation of mono- and tri-layer films is highlighted. In the bulk, T-shaped "rod-coil" molecules without the appended end-groups form predominantly lamellar phases if the core is a straight rod, but the bent-core variety forms hexagonal honeycombs. Furthermore, self-assembly of "Janus"- type molecules, such as those with Y-shaped star mesogens bearing different mutually incompatible side-groups, is discussed. Also covered is the diversity of morphologies observed in miktoarm star terpolymers i.e. polymers with three different and

incompatible arms of well-defined lengths. A range of bulk phases with 3D or 2D order are observed, combining layers, cylinders and cocontinuous networks. Similarities and differences are highlighted between the liquid crystal morphologies on the 3-15 nm scale and the polymer morphologies on the scale 10-100 nm. A separate section is dedicated to computer simulations of such systems, particularly those using dissipative particle and molecular dynamics. Of special interest are the recently synthesised X-shaped tetraphilic molecules, where two different and incompatible side-chains are attached at opposite sides of the rod-like core. The tendency for their phase separation produces LC honeycombs with cells of different compositions that can be represented as paving a plane with different color tiles. The independent variation of chain length and "color" creates the potential for developing a considerable range of complex new 2d- and 3d soft nanostructures. Analogous X-shaped rod-coil compounds with unequal side groups are also of considerable interest, forming tubular lyotropic structures capable of confining strings of guest molecules.

Contents

1 Introduction

Functionality of materials requires order at the nano-scale which in 3D solid state structures and 2D-grids on surfaces[1] can often be described by tessellation (see Figure 1m for the 2D case).[2] Arrays of infinite cylinders with filled or empty pores are examples important for

storage, selective transport or nanopatterning.[3] Solid state structures of this type are usually based on strong interactions, and once formed cannot be changed significantly.[4] In contrast, their soft matter counterparts are amenable to modification by external stimuli. Such soft tessellations have been achieved in polyphilic liquid crystals (LCs)[5] and polymers with star-branched topology.[6,7]

The term polyphilic was coined by Tournilhac et al. for rod-like LCs incorporating perfluorinated segments[8a] and is used here for molecules incorporating more than two incompatible segments.[8,9,10,11,12,13,14,15,16] Here we limit the term to amphiphilic molecules combining three or more distinct incompatible units (mostly ternary and quaternary amphiphiles). While linear polyphilic molecules sometimes show interesting amd unusual morphologies and properties associated with them (e.g. "longitudinal ferroelectric LC",[17] "supramolecular mushrooms",[18] a range of interesting 3D structures in triblock copolymers including double helices[19]), the number of distinct new phase types thus created is relatively limited. In contrast, star-branched polyphiles offer a greater variety of phase structures, as predicted theoretically for star polymers[20] and illustrated on numerous examples of low molecular weight polyphiles and star polymers as discussed below.

This article attempts to summarise recent developments in self assembly of polyphilic star-branched molecules into complex soft matter structures, distinct from simple nematic, lamellar and columnar morphologies usually observed for LC,[21]as well as bring together experiment and simulation. By star-branched polyphiles we mean molecules in which several incompatible moieties are connected close to a central point. These include liquid crystals with side-chain substituted bolaamphiphiles and facial amphiphiles, rods with laterally attached coils, some liquid crystals with star–shaped mesogens and, finally, miktoarm star polymers. i.e. polymers with at least three chemically different arms. The article does not cover linear block copolymers, dendrons or dendrimers, hyperbranched polymers or linear rod-coil molecules. The structures discussed here span a length scale from a few to a hundred nm. One of the aims of the review is, within the above scope, to cross the divide between the liquid crystal and the block-copolymer lengthscales, the two aspects of soft matter self-organization that are usually treated separately. The fundamental concepts of self-assembly of bola- and facial T-shaped polyphilic LCs were outlined previously.[5] Withn this extended-scope, the emphasis of the article is on recent work in the framework of the ESF Eurocores SONS II project SCALES.

The review starts with a brief introduction to T-shaped polyphilic molecules and their liquid crystal structures (section 2.1), with the rest of section 2 covering recent phase structures obtained by molecular design of polyphilic molecules. Section 3 deals with X-shaped amphiphiles, including the preliminary attempts to realize multi-color tiling, i.e. LC honeycombs where the cells are filled by different materials. Sections 4 and 5 review work on the related class of rod-coil molecules with longer rods and bulkier sidegroups and on star-shaped polyphiles, respectively, while section 6 describes the organization of LC amphiphiles on solid and liquid surfaces, including the formation of stable and completely reversible Langmuir films, and their transfer to LB films. Mesostructures with 2D and 3D order in star terpolymers with incompatible arms are reviewed in section 7, where some comparisons with LC polyphiles are made. Computer simulations of the systems covered in the preceding sections, which have been initiated by the reported experimental findings, notably the 2D arrays of polygonal cylinders, are the subject of the 8th section. Future prospects and some potential applications are discussed in section 9.

2 Soft matter structures of ternary T-shaped amphiphiles

2.1 Introduction to self-assembly of T-shaped bola- and facial amphiphiles

In LCs T-shaped block molecules bearing three types of mutually incompatible groups (triphilic, see for example compound **1a** in Figure 1 and compound **2a** in Figure 2) were found to form many fluid self assembled structures, among them a series of honeycombs (e.g. Figure 1c-h).[5]

In these honeycomb LC phases (also described as polygonal cylinder phases) the aromatic rod-like cores form cell walls connected at the "seams" by terminal hydrogen-bonding groups, typically glycerol. The honeycomb cells of polygonal cross-section and infinite length are filled by the fluid lateral chains, typically alkyl chains[22] or semiperfloroalkyl chains.[23] Depending on the ratio of the volume of the chains to the length of the rod-like core, cells ranging from rhombic to hexagonal were obtained.[5,23,24] The sequence of different honeycomb structures observed for these T-shaped bolaamphiphiles (compounds **1**) with increasing length of the lateral chain is outlined in Figure 1c-h. Projected on a Euclidian plane, most observed honeycombs are Archimedean tilings (i.e. tilings in which all vertices, or nodes, are the same - Figure 1m) or their duals.[2,5,24]

Further extension of the lateral chain gives rise to giant cylinder phases (Figure 1g,h).[5,23] In these, some or all cylinder walls have double lengths, being formed by two end-to-end, rather than just one molecule. Further enlargement of the lateral chains leads to the cylinder structure bursting open, giving rise to lamellar phases. Unlike the usual smectic phases, in these lamellar phases the π-conjugated rod-like cores are oriented parallel to the layer plane (denoted hereafter Lam phases). Different modes of orientational and positional order of the aromatic cores are currently under discussion (Figure 1i-l).[5,23,25] We note that some T-shaped compounds display more than one thermotropic phase, and the general trend with increasing temperature is for a compound to undergo a phase transition moving part of the way anticlockwise around the diagrams in Figure 1 and Figure 2.

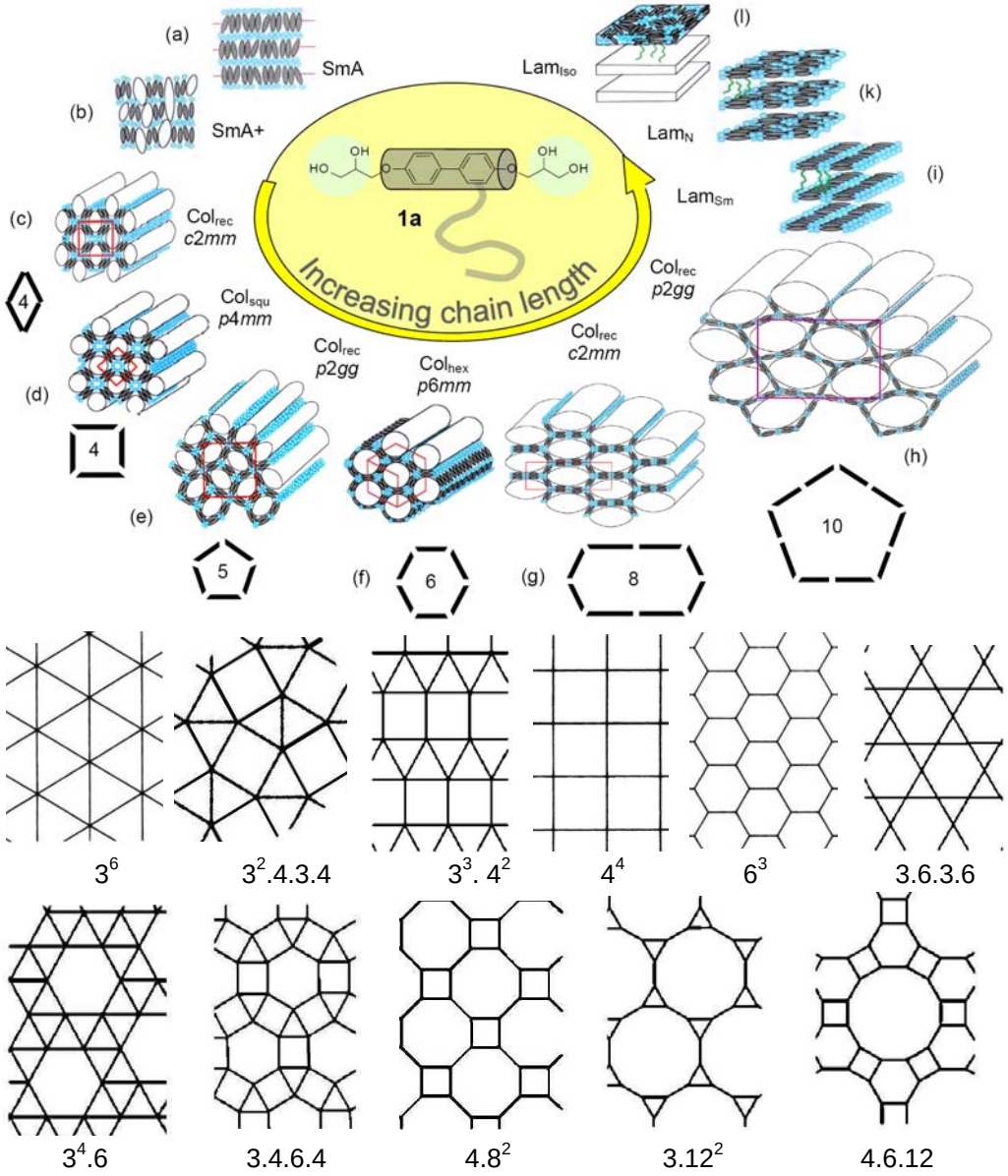

Figure 1. Sequence of LC phases formed by self-assembly of T-shaped bolaamphiphiles (e.g. compound **1a**), depending on the size of the lateral chain: a,b) smectic phases, c-h) polygonal

LC cylinder phases, and i-l) lamellar phases; m) Archimedean tiling patterns[2b,5] ordered according to the size of the largest tiles; those in the first row have been realized either in LC systems[23,27] or in star block copolymers[26] or in both; those in the bottom row have not yet been found in LC systems, but some of them were used to describe polymer morphologies. Reproduced with permission.[5] Copyright 2007, Royal Society of Chemistry.

A related series of complex LC cylinder phases was found for the facial amphiphiles **2,** where the positions of the polar and the lipophilic groups are reversed (see Figure 2).[5,24,27,28,29] However, in addition to the polygonal cylinder phases (Figure 2e-f), different types of filled mesh phases (Figure 2b,c) and channelled layer phases (Figure 2d and n) are also found. In the former the lateral polar chains form clusters within the aromatic layer, positioned either randomly (Figure 2b), or hexagonally ordered within layers and correlated with ABC layer stacking on a rhombohedral lattice (Figure 2c). This phase bears resemblance to the "perforated layer" phase in diblock copolymers, lyotropics or some thermotropic LCs,[30] except that the perforations or "dimples" in the layers are replaced here by a third component, the lateral chains. In the channelled layer (ChL) phases infinite columns penetrate the layers orthogonal to the layer planes. ChL phases are commonly observed in the series of these facial amphiphilic compounds.[5,24,28,29,31] Because in compounds **2** the hydrogen bonding glycerol groups at the ends of the rods are replaced by alkyl chains interacting via weaker van der Waals forces, the stability of the honeycombs is reduced for compounds with relatively short alkyl chains. In such compounds the aromatic cores are not necessarily confined to lie perpendicular to the cylinder axis, but can instead be inclined at a high angle or even be close to parallel to the column axis (Figure 2i,k).[29] Lam Phases (Figure 2l,m) were observed for these molecules only after addition of appropriate polar solvents.[29]

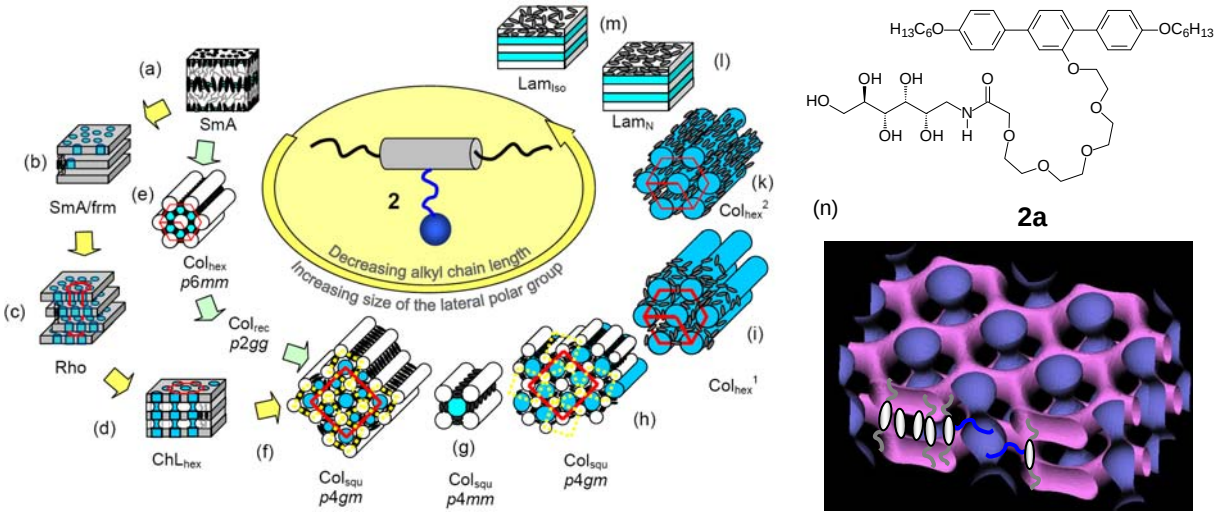

Figure 2. a-m) Phase sequence of the facial amphiphiles (compounds **2**, for a representative molecular structure see **2a**) with increasing size of the lateral substituent and decreasing length of the terminal alkyl chains; n) hexagonal channelled layer phase. Reproduced with permission..[5,31] a-m) Copyright 2007, Royal Society of Chemistry. n) Copyright 2004, Wiley – VCH.

2.2 New types of small cylinder honeycombs

The pentagonal cylinder structure is one of the most exciting LC superstructures reported so far, as periodic tiling of a plane is not possible with regular pentagons.[2,5] However, the liquid crystalline state, combining order and mobility, allows this organization, because it enables the deformation of pentagonal cylinders.[5,24] In this way pentagonal cylinder phases with plane group symmetries *p*2*gg* and *p*4*gm* were observed for these polyphilic LC materials.[5,23,24,28,29]

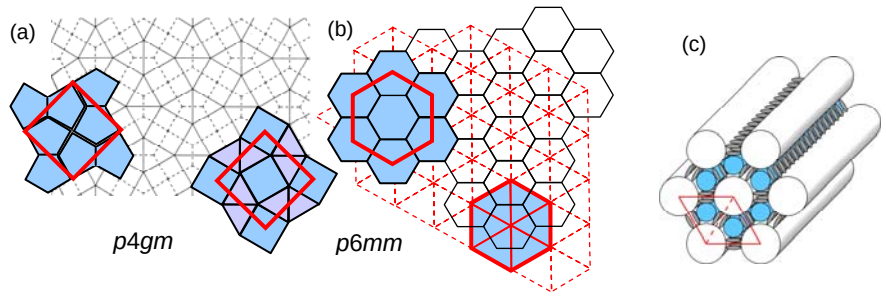

Figure 3. a,b) Topological duals: a) periodic tilings by distorted pentagons and a 1:2 mixture of squares and triangles; b) tilings of regular hexagons and regular triangles; in each pair of tessellations the nodes and tiles are exchanged; for example, in the hexagonal tiling there are threefold nodes and hexagonal tiles, whereas in the topological dual there are triangular tiles and six-fold nodes;[5,24] c) model showing the organization of the facial amphiphiles 2 in the triangular cylinder phase. Reproduced with permission [32] Copyright 2007, American Chemical Society.

From a topological point of view the tiling of a plane by pentagons in the *p*4*gm* lattice is identical to tiling a periodic structure consisting of a 1:2 mixture of squares and triangles. This relationship, known as topological duality, is sketched in Figure 3a.[2,24,5] A dual is created by placing nodes in the ceners of the tiles of the original. The topological dual of the pentagonal cylinder structure, which is a particular arrangement of triangular and square cylinders, was realized as a LC superstructure of terphenyl based facial amphiphiles **2** (e.g. compound **2d** in Figure 4c).[5,24,29] The concept of topological duality was generalized and applied to the design of other new LC superstructures. The hexagonal honeycomb structure, for example, has its topological dual in the tiling by equilateral triangles. LC phases composed of triangular cylinders were obtained with the T-shaped facial amphiphilic three-block molecules **2** with long terminal and short lateral chains (e.g. compound **2b** in Figure 4a).[32]

The trapezoidal cylinder phase (*p*2*gg* symmetry, Figure 4b) is another mode of organization observed for facial amphiphiles, occurring between the triangular phase and the *p*4*gm* lattice composed of squares and triangles.[33] This structure can be regarded as a slightly distorted triangular cylinder phase where the circular alkyl columns are deformed elliptically, thus adding a fourth short side to the triangle. This deformation is attributed to the alkyl chains tending to become more extended and pack parallel to each other at reduced temperatures. In addition, trapezoidal cylinders provide more space for the lateral chains than do triangular ones; hence the phase appears with increase side-chain size between the triangular and the triangle+square *p*4*gm* phase. A phase sequence $Col_{hex}\Delta$/*p*6*mm* (triangles) - Col_{rec}/*p*2*gg* (trapezes) - Col_{squ}/*p*4*gm* (squares+triangles) - Col_{squ}/*p*4*mm* (squares) was for example observed in the series of Li salts **2b-e** by increasing the length of the lateral chain at constant alkyl chain length (Figure 4). A related sequence is observed if the length of the terminal alkyl chains is reduced at constant volume of the lateral chain.[33]

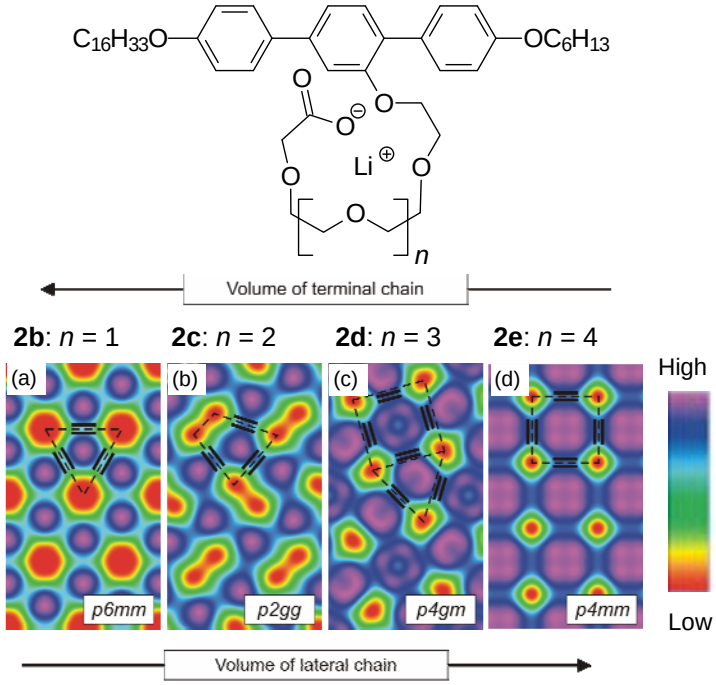

Figure 4. 2D electron density maps of LC phases (view along the column axis) formed by the series of facial amphiphiles **2b-e**, showing the different phase structures developing upon enlarging the lateral chains or upon decreasing the length of the terminal chains: a) $Col_{hex}\Delta$/*p*6*mm* phase composed of triangular cylinders; b) Col_{rec}/*p*2*gg* phase composed trapezoids in which the shortest side is formed by flat alkyl columns; c) Col_{squ}/*p*4*gm* phase composed of a mixture of square and triangular cylinders in the ratio 1: 2 and d) Col_{squ}/*p*4*mm* phase formed by square cylinders. Arrows indicate the direction of increasing volumes of lateral and terminal chains. Reproduced with permission. [33] Copyright 2008, American Chemical Society.

The trapezoidal cylinder phase is distinct from all other honeycomb phases reported so far in that one of the cylinder walls is composed of alkyl chains. These mixed cylinders walls provide three advantages over all-aromatic wall cylinders: (a) they allow improved packing of relatively long alkyl chains at reduced temperature, (b) they provide more interior space than the related triangular cylinders and (c) the space inside the cells can more easily be adjusted to the actual size of the lateral chain. Hence this seems to be the optimal mode of organization for a circumference to area ratio too small for the squares in the *p*4*gm* structure and too large for all-triangular cells. The option of mixed walls further increases the diversity of possible superstructures observed for T-shaped polyphiles. Indeed, recent work shows evidence for trapezoidal cylinders present in combination with all-aromatic cells in some novel highly complex honeycombs (unpublished).

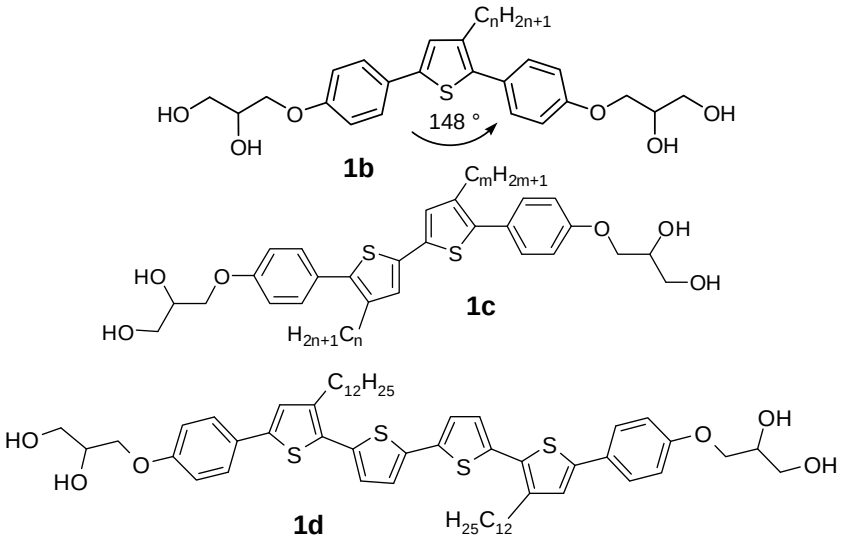

Figure 5 Examples of thiophene-based T-shaped (**1b** and **1c**, if $n = 0$) and X-shaped bolaamphiphiles (**1d** and **1c**, if $n, m \neq 0$).[34,35,36]

Cylinders with triangular and square cross section were recently also obtained for bolaamphiphiles **1** if the length of the rod-like core was increased.[34] This was achieved, for example, by using oligo(thiophene) based π-conjugated cores (compounds **1b-d**, Fig. 5) with only one or two short lateral chains.[34,35,36] For compound **1c** with $m = n = 6$[34] a tiling by triangular cylinder cells was observed ($Col_{hex}\Delta/p6mm$), where the hydrogen bonding networks form the vertices and the interior of the triangular cells is filled with the lipophilic lateral chains. With respect to the position of polar and nonpolar groups, this triangular phase is the inverse of the triangular cylinder phase of the *p*-terphenyl based facial amphiphiles **2**. It should be mentioned here that formation of triangles is additionally favored over larger polygons by molecules having two short chains instead of only one long one of the same total

volume. Thus compound **1c**, with $m = 0$ and $n = 12$ instead of $m = n = 6$, has a *p*4*mm* phase with square cylinders! As the number of chains attached to the rigid backbone has an effect on the thickness of the cylinder walls, this also modifies the space available for the lateral chain.[34]

Such longer rods not only allow cylinder polygons to have fewer sides, but also allow the lateral chains to be attached closer to the centre of the rod. This increases the tendency towards higher symmetry polygons. For example, rhombic cylinders of the biphenyl based compounds **2** were replaced by square cylinders for molecules with longer rods (Figure 6a,b) and for pentagonal cylinder honeycombs the rectangular *p*2*gg* lattice is replaced by the more symmetric square *p*4g*m* lattice composed of less distorted pentagon (Figure 6c,d). Hence, the position of connection between core and lateral chain can modify the phase symmetry at a given net topology.[35]

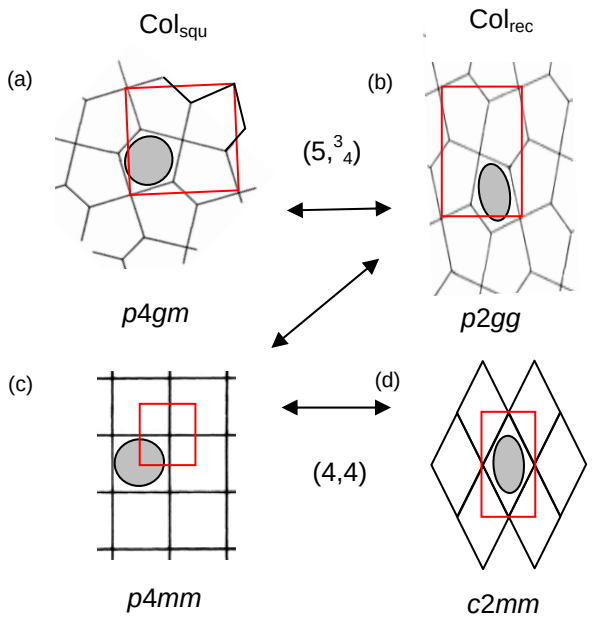

Figure 6. Comparison of symmetries and net topologies of the polygonal cylinder phases formed by the bolaamphiphilic 2,5-diphenylthiophene derivatives **1b** (a,b) and the bolaamphiphilic biphenyl derivatives **1a** (c,d). Reproduced with permission. [35] Copyright 2008, American Chemical Society.

T-shaped polyphiles with extended π-conjugated rods (oligothiophenes,[36,37] but also oligo(p-phenyleneethinylenes),[38,41] are of interest for their luminescent and semiconducting properties and knowledge of the rules of their self assembly could be used to guide their assembly in a predefined way.[39] This could become of importance for the future use of such materials as organic electronic materials.[36,40]

2.3 Polyphiles with bent aromatic cores

Further structural variations result from the introduction of a bend into the aromatic cores. A slight bend (α = 148°) is provided by the thiophene ring in 2,5-diphenyl thiophene based bolaamphiphiles.[35] This bend, though it reduces the mesophase stability, contributes to a reduction of melting points and crystallization tendency, hence widening the mesomorphic ranges. The observed mesophases display cylinder structures very similar to those formed by molecules having strictly linear cores.

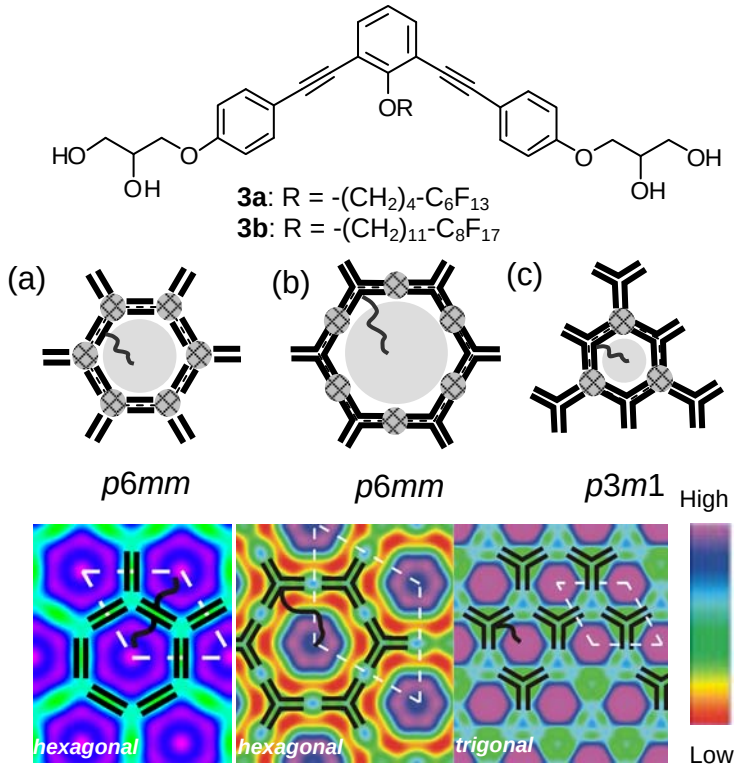

Figure 7. Examples of anchor-shaped (bent-core) bolaamphiphiles **3a**, **3b** and comparison of the hexagonal honeycombs formed by a) linear bolaamphiphiles (compound of type **1**) and b,c) by the two types of bent-core bolaamphiphiles; honeycomb with b) 6-molecule hexagons (*p6mm* symmetry, long side-chain - e.g. **3b**) and c) 3-molecule hexagons (*p3m*1 symmetry, short side-chain - e.g. **3a**); the upper row shows the models and the lower row representative examples of experimental electron density maps for each phase type; in all cases the fluorinated lateral chains inside the cylinders provide the highest electron density (purple). a-c and bottom right: reproduced with permission. [41] Copyright 2008, Wiley – VCH.

A more pronounced effect on phase morphology was observed for aromatic cores with a significant bend, provided by rigid units derived from a 1,3-disubstituted benzene in the anchor shaped bolaamphiphiles **3** (Figure 6).[41] The structures of the LC phases of these molecules are governed by the 120° bend of the aromatic core,[42] which promotes the formation of hexagonal honeycombs. There are two different types of hexagons, 3-hexagons and 6-hexagons (with 3 or 6 molecules in the circumference), leading to LC honeycombs with

*p*3*m*1 and *p6mm* symmetry, respectively (Figure 7b,c). Reducing the volume of the chains leads to a change from larger 6-hexagons to smaller 3-hexagons. The defining parameter is again the ratio between the length of the bent backbone and the volume of the attached chains, i.e. the circumference/area ratio of the polygon, similar to the cylinder phases formed by the linear T-shaped bolaamphiphiles **1**. However, in the cylinder arrays of linear compounds the hydrogen bonding networks are located at all nodes of the honeycomb (Figure 7a). In the *p*3*m*1 phases of compounds **3b** (Figure 7c) only every other node contains glycerol groups, whereas in the *p6mm* phase of compound **3a** (Figure 7b) the glycerols are located in the middle of the walls, and the aromatic cores meet with their 120 deg apices at the nodes. In this respect, the present 6-hexagon structure is the inverse of the hexagonal LC cylinder phases formed by T-shaped molecules.

A further feature of the large 6-hexagon honeycomb is the nano-phase segregation within the cylinders. The fluorinated segments congregate in the centre (blue-purple in the middle map in Figure 8), while the lowest electron density alkyl spacers line the interior of the cylinder walls (red). This core-shell structure is a common feature of a number of honeycomb phases containing ≥6 perfluorinated carbons in the side-chain – see e.g. Figure 8.

It should be stressed that the 3-hexagon honeycomb has broken symmetry, the plane group *p*3*m*1 not having a center of inversion. Hence this, to our knowledge first documented trigonal columnar phase, should have nonlinear optical properties.[43]

2.4 T-shaped molecules with extended lateral groups - From hexagonal cylinders via giant cylinders and lamellar phases to rod-bundle phases

In a different set of studies attention was focussed on increasing the size of the cylinders beyond the hexagonal ones. This was achieved (i) by replacing alkyl chains by semiperfluorinated chains,[5,23,25,44] (ii) by introducing bulky oligosiloxane or carbosilane side-chains,[45] (iii) by replacing linear chains with branched ones (swallow tailed lateral chains)[46,47] or (iv) by attaching bulky end groups to these chains.[46] as well as by (v) using more than one chain attached to the aromatic core.[34,36,47,48] Examples of molecules investigated in this respect, together with their phase types reported in the references given and as shown for selected examples in Figure 8 and Figure 9.

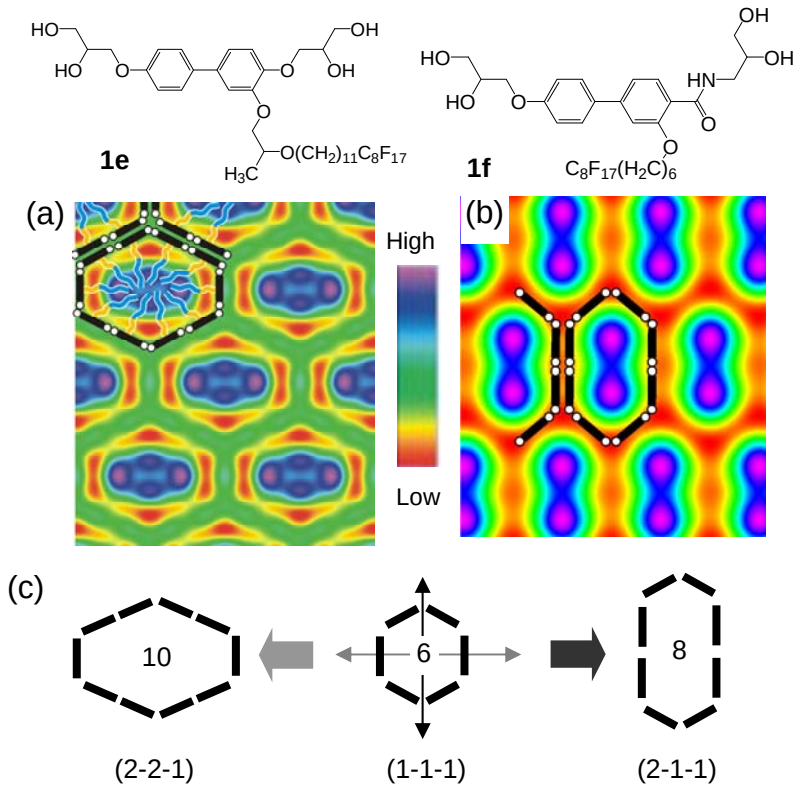

Figure 8. Comparison of the two different types of giant hexagon cylinder structures of compounds **1e** (hexagons with 10 molecules in circumference, 2-2-1, left column) and **1f** (hexagons with 8 molecules in circumference, 2-1-1, right column): a,b) electron density maps reconstructed from powder X-ray patterns; c) shows how stretching of regular hexagonal cylinders (1-1-1) of a Col_{hex} phase either perpendicular to a side or along a diagonal gives rise to two different cylinder phases with *c*2*mm* symmetry (cf. Figure 20). a,c) Reproduced with permission. [44,49] a,c) Copyright 2007, Wiley – VCH. b) Copyright 2010, Institute of Physics.

Increasing the length of the fluorinated segment in the lateral chain of biphenyl based bolaamphiphiles **1a** leads to two types of giant cylinder phases with *c*2*mm* symmetry formed by elongated hexagons with, respectively, 8[23a] and 10 biphenyl cores,[44] arranged around the circumference of each core-shell-column . Figure 8a,b shows electron density maps in cross-section normal to the 8- and 10-hexagon cylinders, with schematic molecular cores (black) overlaid. 3D models of the two phases are shown in Figure 20 further below. Three adjacent sides of a 10-hexagon contain, respectively, 2, 2 and 1 molecules lengthwise, hence this structure is labelled 2-2-1. By analogy the 8-hexagons are labelled 2-1-1.[44,49] Giant pentagonal cylinders, where each side contains two end-to-end molecules, represent another mode of organization of ten molecules in the circumference (see Figure 1h).[23a] Increasing temperature or further enlargement of the lateral chain volume causes the cylinders to burst; the side walls are removed leaving only disconnected layers.[44] In the two lamellar phases adjacent to the polygonal cylinder phases (Lam_{Sm} and Lam_N) the biphenyl cores remain

parallel to the layer planes before the in-plane molecular order is lost in the Lam_{Iso} phase (see Figure 4b).[23,25,44,45,46]

Further increasing the volume of the lateral chains can lead to the break-up of the infinite rafts of bolaamphiphiles into laterally isolated bundles. These pack on a hexagonal lattice, creating a unique type of columnar LC phase (see Figure 9).[46,47]

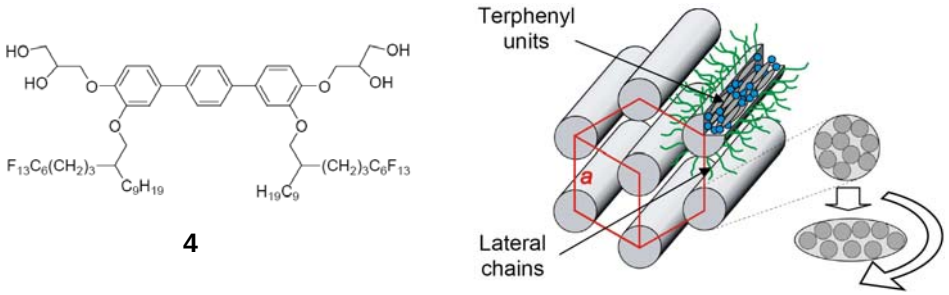

Figure 9. Rod-bundle phase formed by compound **4**; the instantaneous local cross-section of the columns is thought to be elliptical, but circular when averaged over time and space, hence leading to 2D hexagonal symmetry. Reproduced with permission.[47] Copyright 2008, American Chemical Society.

In these rod-bundle phases the birefringence is positive (π-conjugated aromatics are parallel to the columns) whereas it is negative in the polygonal cylinder phases (π-conjugated aromatics perpendicular to columns). On lowering the temperature a Bragg diffraction peak appears corresponding to the spacing identical to the bolaamphiphile length. This signifies the transition to a 3D ordered phase in which intercolumnar long-range correlation is established between the, probably already existing, aromatic and glycerol columnar segments (Figure 9). Regarding the nature of the low-temperature phase, although there is 3D long range order in density fluctuations, we still regard it as liquid crystalline, since there is no preferred position for the individual molecules within a bundle (hence the diffuse wide-angle X-ray scattering).[47]

As in the case of other amphiphiles the lamellar phases (Lam) and the two different types of columnar phases - the rod-bundle phases with positive mean curvature of the aromatic-aliphatic interface, and the polygonal cylinder phases with negative curvature - are separated by numerous different types of intermediate phases, such as bicontinuous cubic phases which are presently under investigation.[50] This to an extent parallels the behavior of lyotropic LCs[51] and block copolymers,[6] or indeed polycatenar[52] and taper-shaped thermotropics.[53,54] However, the diversity of the intermediate phases in the presently discussed polyhiphiles appears to exceed that in other soft matter systems.

Beside chain fluorination and chain branching (swallow tail substituents), siloxane and carbosilanes also represent appropriate building blocks for T-shaped polyphiles with increased volume of the lateral chains. These Si-containing polyphiles display transitions to Lam and rod-bundle phases similar to those described above.[45]

3 X-shaped polyphiles – Approaching multi-color tilings

3.1 Cylinders with single molecule walls

Attaching only one lateral chain to the rod-like core (T-shaped amphiphiles **1a-f**) gave rise to LC cylinder phases where the cross-section of the cylinder walls contains two rods arranged side-by-side, i.e. the cylinders have double walls (Figure 10a,b).[34,48] However, by attaching two lateral chains at opposite sides of the aromatic core (X-shaped polyphiles, compounds **5,6**) generates polygonal honeycombs with walls that are only one molecule thick (Figure 10d,e). This is because it is sterically unfavorable for the second chain to enter the same cell as the first. However, if one assumes the usual molecular spacing of 0.45 nm along the cylinder axis, then the wall thickness comes out as not exactly 1.0, but rather a value between 1.1 and 1.5. This indicates a staggered arrangement of the aromatic cores (Figure 10c), This arrangement seems to maximize the interactions between the aromatic cores, while allowing sufficient space for the lateral chains to enter the interior of the cells.[34,48] As a consequence of the thinner cylinder walls effectively more space is left available for the lateral chains inside the cells. Hence, honeycombs with smaller cells could be achieved by using two short chains instead of only one chain with the same total volume.[34]

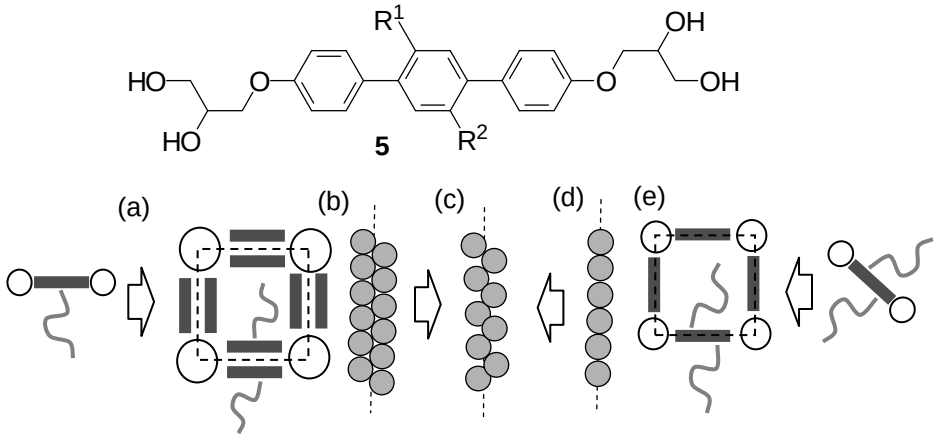

Figure 10. Dependence of wall thickness on the number of lateral chains on the example of square honeycombs: a,e) cuts across one cylinder; b-d) cuts through a cylinder wall along the cylinder axis; a,b) double wall structure of T-shaped bolaamphiphiles; d,e) single wall cylinders formed by X-shaped molecules, and c) staggered arrangement of the aromatic cores

as found in practice for the honeycombs of X-shaped compound like **5** (R^1,R^2 = OC_mH_{2m+1}, $O(CH_2)_pC_nF_{2n+1}$).[34,48] Reproduced with permission.[34] Copyright 2009, Wiley – VCH.

3.2 X-shaped tetraphiles – The two-color liquid crystal kagome

Attaching two different chains, R_1 and R_2, either to the same ring at opposite sides (as in compound **6** in Figure 11) or to different rings of the same core, offers the possibility of creating liquid crystalline honeycombs with cells of different composition. If projected on a Euclidian plane, such a structure can be described as tiling by two or even more different color tiles (multi-color tiling patterns). The two color kagome of the specifically designed compound **6** is an example.[55] In this compound R_1 is an aliphatic hydrocarbon chain and R_2 a semiperfluorinated chain with very different volume, were affixed to an elongated oligo(phenylene ethinylene) based bolaamphiphilic core, terminated by glycerol groups. Hence, this compound represents a Janus-type[56] X-shaped tetraphile (quaternary amphiphiles). This compound forms a hexagonal columnar phase (Col_{hex}/*p6mm*) with a lattice parameter corresponding to approximately twice the length of the rigid bolaamphiphilic moiety – see Figure 11. This suggests a kagome lattice, the 3.6.3.6 trihexagonal tiling of hexagons and triangles of equal side lengths. The kagome lattice was indeed confirmed by electron density map reconstruction – see Figure 11b. Moreover, the map also shows that the hexagons are high density (purple/blue), i.e. containing the semiperfluorinated chains, while the triangles are low density (red), containing the non-fluorinated alkyl chains. Such distribution is to be expected from a compound with a long fluorinated and a short alkyl side-chain as, in an idealized kagome, the overall hexagon/triangle area ratio is 3:1. The structure is clear from the dynamically annealed molecular model in Figure 11c, where the aromatic+glycerol, aliphatic and fluorinated moieties are colored green, red and blue, respectively (periodic boundary box equal to one unit cell only). The initial (random) and final (ordered) arrangement of stylized T-shaped molecules using a large scale DPD simulation are shown for comparison in Figure 11d – for details see section 8.[55]

This represents the most complex structure reported so far in LC phases of polyphilic molecules and paves the way to a series of new and even more complex types of LC phases, described by multicolor tilings, i.e. with nonequal composition of the interior of neighbouring cells. A range of LC honeycombs with interesting tiling patterns and with cells of up to 5 different R_1/R_2 ratios (colors) and 4 different shapes have been generated recently.[57] This includes some of the structures discussed in section 8, such as that in Figure 34. The

complexity is brought about by the competition between conflicting requirements for phase separation and space filling.

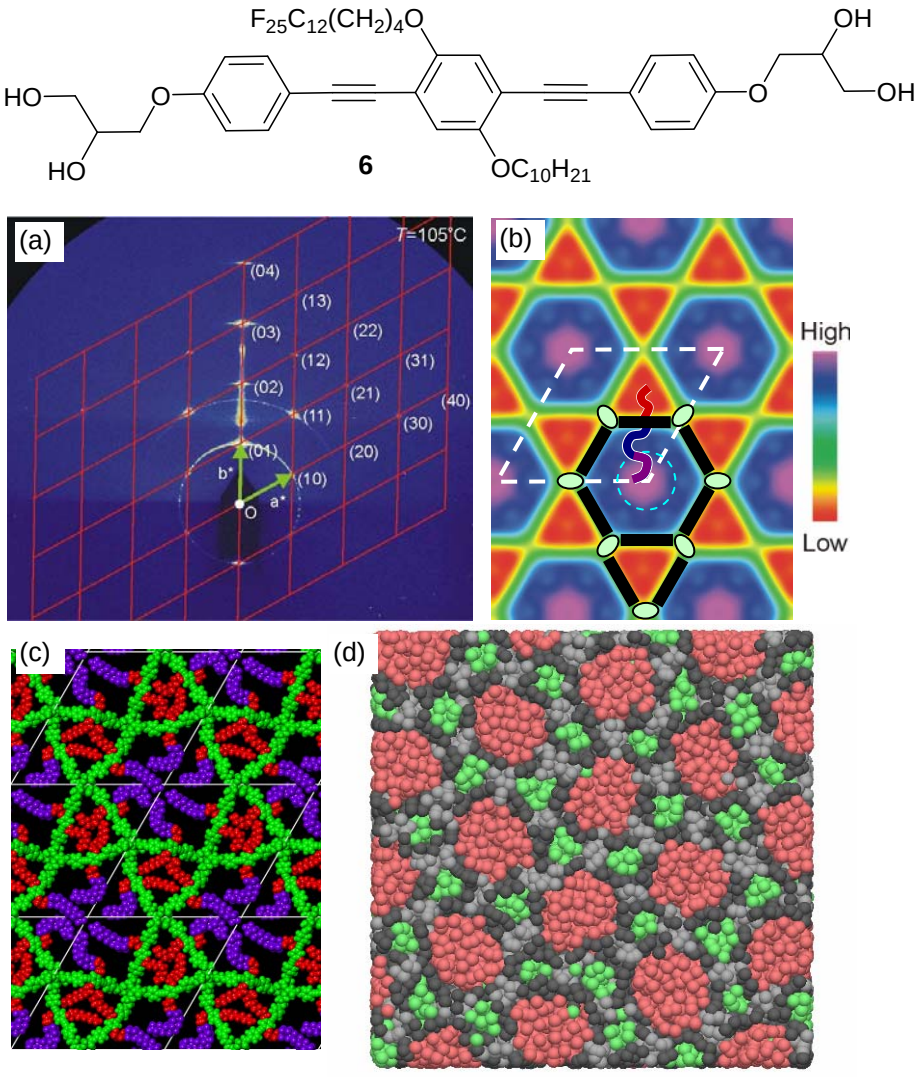

Figure 11. a) GISAXS pattern of compound **6** on Si surface; the reciprocal net is superimposed; b) electron density map calculated from powder diffraction pattern; the schematics of rod-like aromatic cores of eight molecules are overlaid (black lines) with their terminal glycerol groups (white ellipses); one of the cores has its two lateral chains drawn; c) snapshot of an atomistic model after molecular dynamics annealing (box equal to experimental unit cell with c = 0.45 nm, with periodic boundary conditions); d) snapshot of a DPD simulation where the individual beads represent groups of atoms; here the stiff "aromatic" cores are dark grey and the flexible "alkyls" are green (for details see section 8). b-d) Reproduced with permission. [55] Copyright 2008, Wiley – VCH.

4 T-shaped, X-shaped and anchor-shaped rod-coil molecules without terminal chains

"Rod-coil" molecules is one of the areas where block-copolymers and low-molecular thermotropic liquid crystals come close together. The term is used predominantly to describe block- or star-copolymers in which some blocks (arms) are rigid while others are

flexible.[18,58,59] There is currently considerable interest in rod-coil block copolymers, their prospective area of application primarily being determined by the nature of the rigid block. E.g. copolymers containing aromatic polyester blocks for structural applications, π-conjugated blocks for nanopatterned electronic and optoelectronic devices,[60,61] and those with e.g. polypeptide α–helical or β-sheet blocks in biomedical applications.[62] Rigidity of a block can also be achieved by jacketing or "dendronizing" a flexible backbone.[63] The introduction of rod-like blocks drastically changes the thermodynamics (entropy) of the system, and in order to describe the systems physically, anisotropic interaction has to be considered, e.g. using a mean field (Maier-Saupe) theory.[64] In most rod-coil compounds the blocks are linked end-to-end, and in such systems some interesting phase morphologies were found in simulations[65] and experiment, incuding undulated lamellae, 3D phases (e.g. body-centered tetragonal, hollow cylinders and spheres (vesicles) in solution.[58,66,67,68] However, in this article we concentrate on molecules where the coils are tethered to the side of the rigid block.

Recently Lee et al. synthesised T-shaped and X-shaped amphiphiles, having longer rigid cores and bulkier flexible groups compared to those in the LCs described in sections 2-4. Also, these cores did not contain the additional end groups. Bulk solid state properties were studied, as was their self assembly in aqueous systems.[69,70,71,72] T-shaped facial amphiphiles **7a,b** form stepped strips in the solid state (Figure 12).[69] The rod segments within the strips are aligned parallel to each other to form discrete sheets which subsequently stack together with a partial overlap to form a stepped 1D structure. The rod segments are arranged parallel to the strip axis. The interdigitation of the rod-ends is most likely due to the absence of attractive interactions at the molecular ends which would inhibit sliding of the rods over each other.

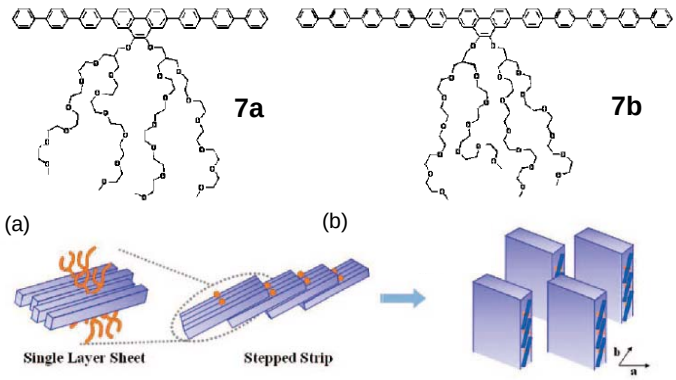

Figure 12. T-shaped rod-coil molecules **7a** and **7b** with oligo(p-phenylene) rods of different length and branched polar oligo(ethylene oxide) groups forming stepped stripes which organize on a 2D oblique lattice. Reproduced with permission [69] Copyright 2008, American Chemical Society.

Overlap of the rods can be reduced by reducing the rod-length or by increasing the size of the lateral flexible units. Laterally grafted rod-like amphiphiles have also been synthesised carrying a hydrophilic oligo(ethylene oxide) based dendron at one side and a hydrophobic brush of alkyl chains at the opposite side (X-shaped ternary amphiphiles **7c,d**, see Figure 13). These were found to form sheet-like structures with in-plane anisotropy (Lam_N or Lam_{Sm}-like structures) in aqueous solutions.[70] The anisotropic sheets, upon heating, spontaneously roll up along the direction of the rod axis to form tubular scrolls. This unique structural transformation is thought to arise from the in-plane orientational order of the rod segments in which the rods are arranged parallel to the sheet planes.

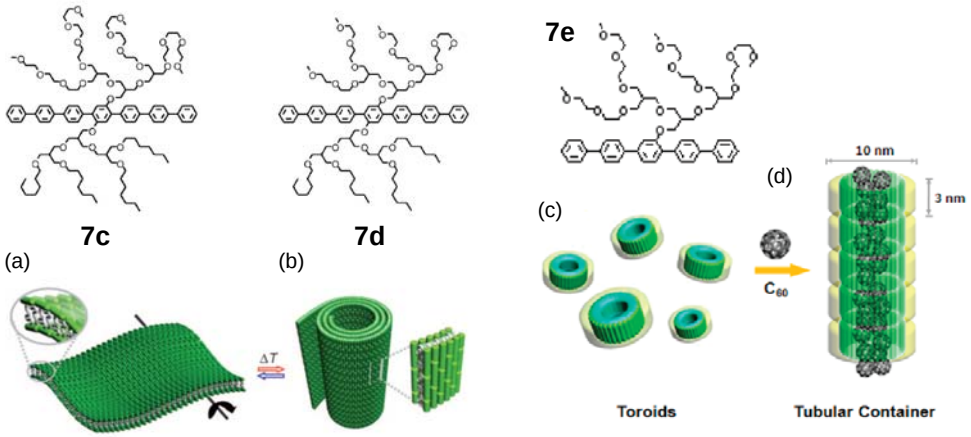

Figure 13. Self assembly of X-shaped rod-coil molecules **7c** and **7d** having a dendritic and hydrophilic oligo(ethylene oxide) side group and a hydrophobic brush with n-alkyl end chains in excess water: a) anisotropic planar sheets and b) scrolling of these sheets to tubules as observed for compounds **7c** and **7d**; c) toroids formed by aqueous self assembly of mixtures of the X-shaped compounds **7c** and **7d** with the T-shaped molecule **7e** and d) formation of tubules from these toroids encapsulating fullerene molecules. Reproduced with permission.[70a, 71] Copyright 2009, Wiley – VCH and 2009, American Chemical Society.

Diluting these X-shaped amphiphiles by the T-shaped facial amphiphile **7e** leads to toroids with a hydrophobic cavity, a hydrophilic exterior and a height corresponding to the length of the rod-like building blocks (Figure 13c).[71] This structural transformation from planar sheets via elongated cylinders to discrete toroids upon addition of **7c** can be explained by the increasing volume fraction of hydrophilic segments through co-assembly. With increasing content of **7e**, which contains only one hydrophilic brush, the 2D sheets dissociate into smaller aggregates, allowing the increased number of oligoether chains to escape confinement without sacrificing the anisotropic packing of the rod segments. The axis of curvature of these lamellar aggregates is parallel to the long axis of the rods, leading to the formation of toroids. The toroids can stack into tubules triggered by guest (C_{60}) encapsulation (Figure 13d) through hydrophobic interaction of the C_{60} fullerene with the hydrophobic interior of the toroids.[71]

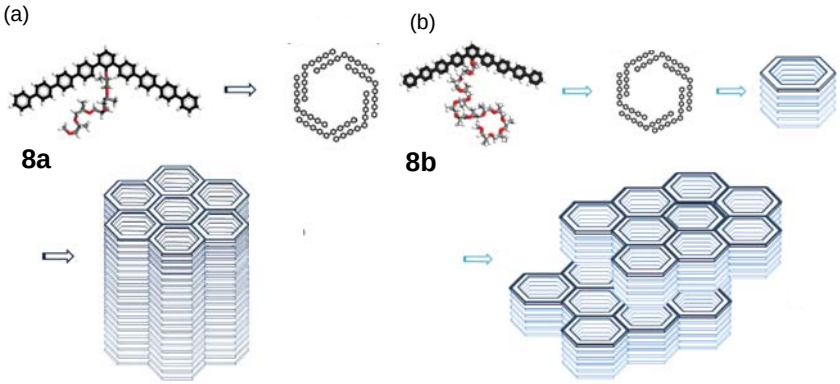

Figure 14. Bulk self-assembly of anchor shaped rod-coil molecules **8a** and 8b: a) into a 2D hexagonal channel structure and b) formation of hexagonal honeycomb meshes by extension of the lateral oligo(propylene oxide) chain. Reproduced with permission.[72] Copyright 2008, American Chemical Society.

Bent-rod molecules like **8a** (Figure 14a) with a relatively short oligo(propylene oxide) chain self-assemble into a hexagonal homeycomb structure, similar to that reported for the anchor shaped molecules **3** (see section 2.3).[72] Within the channels, six bent rods self-assemble into hexameric macrocycles that stack on one another to form a honeycomb of channel-like columns where the interiors are filled by the flexible oligo(propylene oxide) chains (Figure 14a). However, the absence of hydrogen bonding at the ends of the aromatic cores leads in this case to intercalation of the aromatics in the cylinder walls (Figure 14a). Furthermore, the absence of hydrogen bonding along the cylinders also allows easy break up of the honeycomb into discrete hexagonal mesh layers (Figure 14b). This takes place by increasing the length of the lateral oligo(propylene oxide) chain (compound **8b**), leading to an overcrowded cell filling which interrupts the infinite honeycombs into hexagonal honeycomb layers with well defined height. A further increase in the length of the flexible chain induces lamellar organization,[72] similar to that in the Lam phases.[5,23,25]

5 Polyphilic liquid crystals with other molecular topologies

Though not in the direct focus of this feature article, selected examples of complex liquid crystal phases formed by other types of polyphilic molecules are also worth mentioning. One such example is the group of star branched oligobenzoates having two or even three different and incompatible types of chains attached to the Y-shaped[73] branched aromatic core (Figure 15). Compounds **9** and **10** show complex columnar mesophases at low temperature and lamellar phases (SmA) at higher temperature.[74] The SmA phase results from the segregation of the fluorinated chains into distinct layers, separate from the layers formed by the hydrocarbon parts of the molecules. The aromatic columns in the hydrocarbon layers adopt

only short range correlation and hence a long range positional correlation of the columns in adjacent layers is not achieved (Figure 16a).[75] Only at reduced temperature is long range order of the aromatic columns established, which in the case of compound **9** leads to a 2D lattice with the unusual plane group symmetry *p2mg* (Figure 16b). Formation of lamellar LC phases, due to the segregation of fluorinated chains into separate R_F-layers, was also reported for disc-like molecules substituted with aliphatic and fluorinated chains.[76] Janietz et al. reported hydrogen bonded complexes between benzoic acids with two or three semi-perfluorinated chains and alkyl substituted melamines. These can be regarded as supramolecular stars. For complex **11** (Figure 15) the R_F chains are organized in separate columns.[77] As the periodicity of the positions of the R_F columns is larger than the periodicity of the main columns formed by the aromatic cores, a hexagonal columnar superlattice structure was proposed.

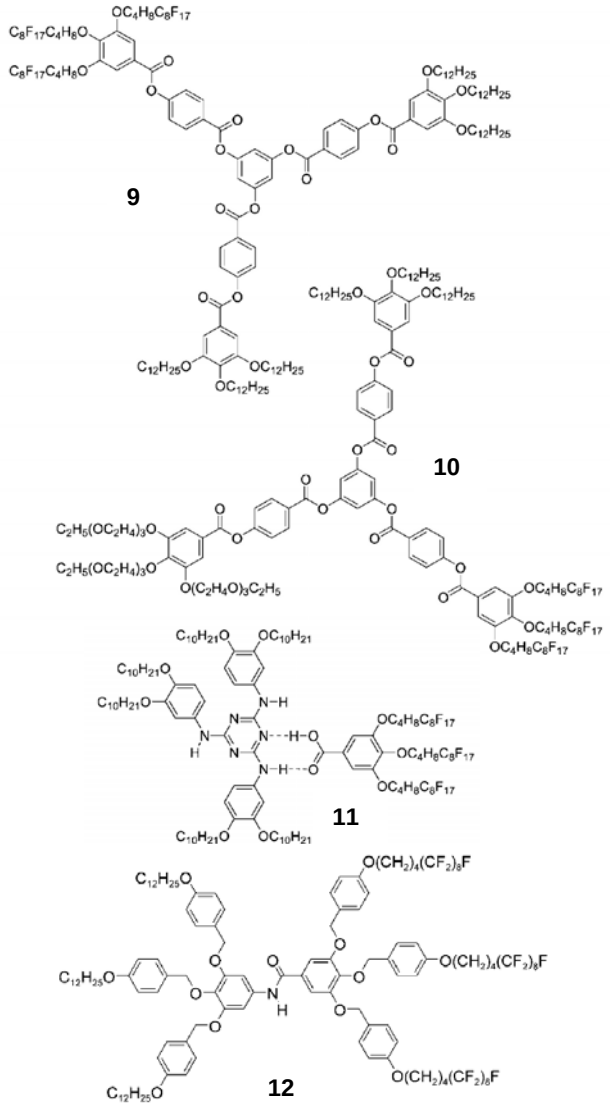

Figure 15 Figure 15. Examples of polyphilic molecules with star shaped molecular topologies.[74,77,78]

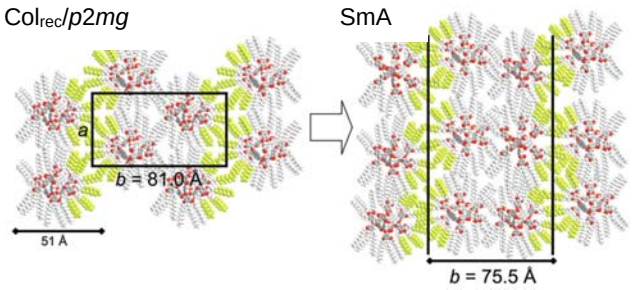

Figure 16. Examples of superlattice LC phases formed by the Janus-type star shaped compound similar to 9 (cross section through the structure viewed along the column axis). Reproduced with permission.[74a] Copyright 2008, Royal Society of Chemistry.

Percec et al. descibed the self-assembly of R_F-substituted bis-dendritic benzamides such as compound **12** (Figure 15) combining a dendron decorated with perfluorinated chains and a dendron with alkyl chains. In the hexagonal columnar LC phases of these molecules the smaller alkyl chains form the centers of the columns, the aromatics are arranged in cylindrical shells surrounding the aliphatic columns, while the larger fluorinated chains form a fluorous continuum around the core-shell columns (Figure 18b).[78] Another kind of core-shell columnar phase was obtained for ionic LCs composed of a rod-like imidazolium salt with a short single alkyl chain at the ionic end and three long alkyl chains attached to the non-ionic end.[79] The short chains form the cores, the aromatics form the shells and these core-shell columns are embedded in the continuum of the long flexible chains (Figure 17 and Figure 18c). In this case the self-sorting of the alkyl chains is driven by the incompatibility and segregation of the ionic ends of the rods, forming the inner surfaces of the aromatic shells, from the non-ionic ends, forming the outer surfaces. However, for compounds **13** not only core-shell columns, but also core-shell spheroids were obtained (Figure 17).[79] These thermotropic bulk structures, where the aromatic walls enclose the same material as that in the surrounding continuum, are in some respect related to vesicles formed by simple amphiphiles in aqueous solution. This kind of columnar phase was previously suggested by Levelut et al. and assigned as “complex columnar phase”.[80]

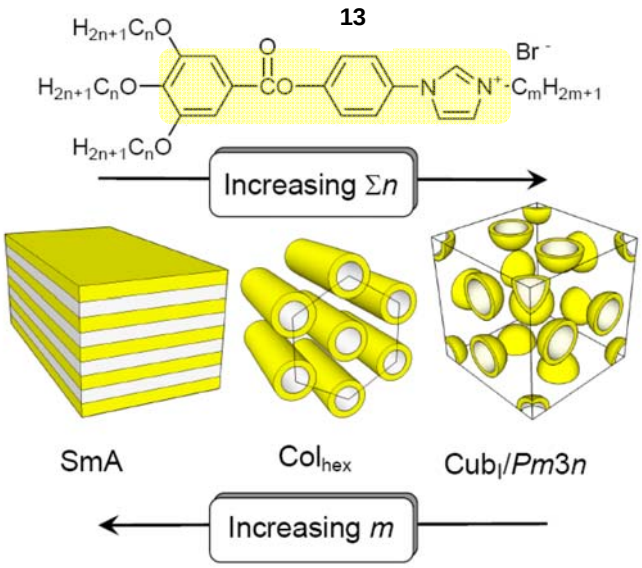

Figure 17. Self-assembly of polycatenar imidazolium salts **13** into "vesicle-like" columnar and micellar cubic phases, where the aromatic imidazolium based cores form the shells. Reproduced with permission. [79] Copyright 2010, Wiley – VCH.

Similar types of core-shell columns and core-shell spheroids, with aromatic units separating inner and outer lipophilic regions, were recently also reported by Percec et al. for taper-shaped amphiphilic molecules.[81] Interestingly the material inside and outside the aromatic shell are identical aliphatic chains, the vesicle-like structure driven entirely by the shape of the tapered molecules,. Here the aromatic wall is an asymmetric partially interdigitated bilayer, whereas the vesicle wall in the imidazolium salts **13** have monolayer structures. There is also a relation between these vesicle-like phases and the honeycomb LC phases discussed in section 3, as in both cases the aromatic parts form cylinders. However, in contrast to the polygonal honeycomb phases (Figure 18f) the aromatic cylinder walls in the vesicle-like phases are not interconnected to form a honeycomb network, but are separated by a fluid continuum which represents a honeycomb itself (Figure 18c). Nevertheless, recent work has shown that these isolated cylinders can also adopt a polygonal (hexagonal or square) shape (Figure 18d) due to packing constraints.[81] It is worth mentioning that a helical columnar phase with a true void in the column centre has in fact been found in thermotropic alkyl-substituted helicenes, due to the inability of the blunt tip of the molecule to reach the centre of the column.[82]

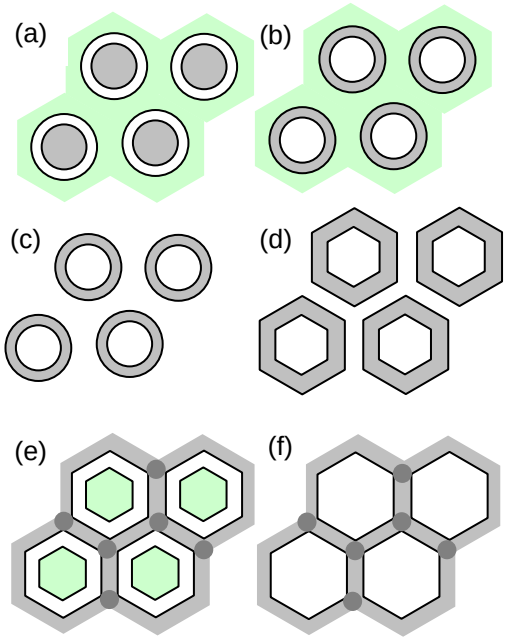

Figure 18. Comparison of LC core-shell structures (upper line), vesicle-like LC phases (middle line) and polygonal honeycomb LC phases (lower line): a) core-shell structure with aromatic cores and aliphatic corona in a fluorous continuum; b) core-shell structures with aromatic shells; c,d) vesicle-like columnar phases, c) with circular and d) hexagonal cylinders; e,f) polygonal honeycomb phases e) with core-shell structure and f) with uniform cells. View along column axis. Color code: light gray = aromatic, white = aliphatic, green = R_F chains (these regions could alternatively contain oligosiloxanes or ionic/non-ionic polar groups); dark grey = positions of the hydrogen bonding networks in the honeycombs.

Polyphilic molecules, where the incompatible chains are fixed at opposite sides of a central core could be regarded as Janus-type molecules. In addition to compounds **9-12** there are several other types of Janus mesogens, such as oligomesogens[83,84] and dendrimers incorporating different types of rod-like segments[85,86] or combining rod-like and disc-like units.[87] However, segregation of the two faces of these molecules, leading to a distinct LC phase structure, does not occur in all reported cases.

In another type of polyphilic molecules the fluorinated segments are connected to an aromatic or polar core via relatively long alkyl chains. For these compounds segregation of the hydrocarbon spacers and fluorinated ends leads to core-shell structures with aromatic column cores and aliphatic shells embedded in a fluorous continuum[88] (Figure 18a). This type of core-shell morphologies can be regarded as inverted with respect to those found for the bis-dendron **12** (Figure 18b) as the positions of aromatic and hydrocarbon regions is exchanged. They are also inverted with respect to core-shell honeycombs shown in Figure 8 and Figure 18e as the positions of fluorinated and aromatic regions are exchanged.

While the discussion in this section focussed mainly on polyphiles incorporating fluorinated segments, oligosiloxane segments[89] and polar groups[90] can also lead to related core-shell and super-lattice columnar structures.

6 Self-assembly of T-shaped and X-shaped polyphiles at interfaces

6.1 Alignment of thermotropic phases on substrates

Alignment of liquid crystals on surfaces is, of course, a well studied subject as it is crucial for the operation of LC displays and most other LC applications – see e.g. [91,92,93,94]. Planar alignment with the director parallel to a preferred direction is traditionally achieved for nematics and smectics by rubbing a polyimide-coated substrate, while homeotropic (vertical) alignment can sometimes be achieved by treating the glass or Si surface with alkylsilanes or quaternary ammonium salt with a long alkyl chain, or similar surfactants. Alignment of columnar phases is usually less controllable. Recent studies of surface alignment of discotic columnar LCs, such as hexaalkoxytriphenylenes, established that planar alignment is favored by the LC-air interface, while homeotropic alignment is favored by the LC interface with substrates such as glass, ITO and silicon.[95] In terms of surface energies:

$$\gamma_{\text{LC-air}} >> \gamma_{\text{LC-solid}} > \gamma_{\text{LC-iso}}$$

The reason for the high $\gamma_{\text{LC-air}}$ is thought to be the high energy of breaking the polarizable π-system at the air surface.[96] On the other hand, homeotropic alignment, which is preferred in many applications of discotics, was thought to be often kinetically favored on solid substrates due to the seed orientation, so that this alignment could be trapped even if the equilibrium favors planar orientation. Work on self-assembled columnar phases of wedge-shaped and dendritic mesogens has shown that fluorination of the alkyl chains stabilizes homeotropic alignment on solid substrates.[97] It has been shown recently that nanopatterning discotic columnar LC in stripes by dewetting on silicon substrate can lead to controlled planar alignment where the columns are preferentially oriented either along or normal to the stripes, depending on the mesogen used.[98] The orientation is probably affected by the direction of the curvature of the LC-air interface.

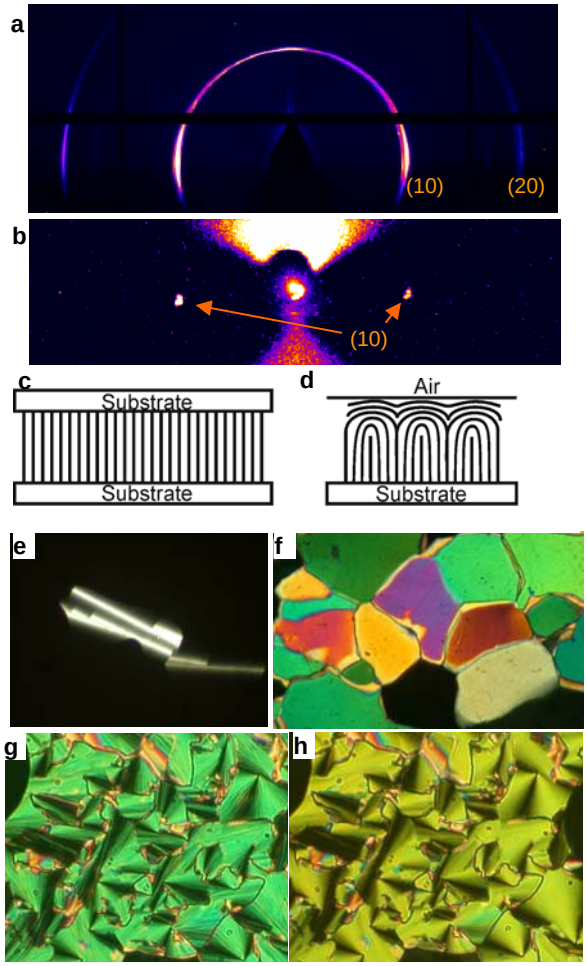

Figure 19. a) GISAXS pattern of the hexagonal honeycomb phase of a T-shaped bolaamphiphile with a semifluorinated side chain – uncovered film on Si wafer; b) GISAXS of a film of the same compound sandwiched between two Si wafers; c) cross-section through the sandwich in (b) showing column director lines (schematic); cross-section of the sample in (a). e) 360° tumbling defect in an otherwise homeotropic hexagonal honeycomb of a bolaamphiphile with a carbosilane side chain;[45] f) mosaic texture of the 3D-orederd ChL_{hex} (hexagonal channeled layer) phase of a facial T-shape amphiphile;[31] g) fan texture of a facial amphiphile in the hexagonal honeycomb phase;[33] h) the same sample at lower temperature in the trapezoidal honeycomb phase with rectangular *p*2*gg* symmetry. [33]

Surface alignment experiments with honeycomb columnar phases of T-shaped amphiphiles parallel the behaviour of the discotics to a large extent. This is perhaps not surprising cinsidering that the π–π interaction also extends along the cylinder axis through the aromatic stacks in the honeycomb walls. Figure 19a shows the Grazing incidence X-ray diffraction (GISAXS) pattern of an uncovered hexagonal honeycomb LC film of a bolaamphiphile with a semiperfluorinated alkyl side-chain on horizontal Si surface.[99] The (10) diffraction arc has intensity maxima on the equator, coming from the homeotropic alignment, but the arcs extend to the meridian, where another weak maximum indicates planar aligment. However when the

film is sandwiched between two Si wafers, the alignment is purely and perfectly homeotropic, as demonstrated by the very sharp and localized equatorial spots in Figure 19b. The corresponding alignment profile of the hexagonal cylinders for this latter case is shown schematically in Figure 19c, while that for the uncovered film is depicted in Figure 19d. The homeotropically aligned T- and X-shaped compounds between two glass slides are often seen to display tumbling defects similar to those in Figure 19d. Figure 19e shows such a defect, but the dark line in the middle suggests that here the director performs a 360° turn.

Colors appear when the LC film thickness d (in μm) is large enough, i.e. when

$$d > \frac{\lambda_{\min}}{|n_e - n_o|} \cong \frac{0.3}{|n_e - n_o|}$$

where n_e and n_o are the extraordinary and ordinary refractive indices and λ_{min} is the shortest visible wavelength. The colors are instructive as they hold information on the director inclination to the substrate surface, in contrast to brightness, which is related to in-plane orientation relative to the polarizers. Thus in the fan texture in Figure 19g the hexagonal honeycomb cylinders are parallel to the substrate almost everywhere, i.e. wherever the color is green. On cooling by a couple of degrees the phase of this facial amphiphile changes to a rectangular columnar with trapezoidal cylinders, described in section 2.2.[33] The color changes to a fairly uniform yellow (Figure 19h), which means that $|n_e - n_o|$ had decreased. Since the indicatrix of the rectangular phase is biaxial, the uniformity of the yellow now implies not only that the column long (z) axis remains in the plane of the film, but that the x and y axes also maintain a uniform inclination to the surface.

The situation with surface alignment of LC phases with 3D order can be more complicated, as found for the channeled layer (ChL_{hex}) phase of facial amphiphiles (cf. Figure 2n).[31] Figure 19f shows the mosaic texture of this phase, with different mosaic domains displaying different colors; this includes black that is invariant to sample rotation, hence coming from homeotropic domains. The difference in color originates in variation in optic axis (i.e. director) inclination to the film surface. This ambivalence in director inclination presumably results from the opposing tendencies for either the layers or the channels to align parallel to the surface. In fact, it is most likely that, while the black domains sit on {001} planes, those of other colors sit on a selection of only a few favorable crystallographic {hkl} planes; hence only a few colors recur.

While optical microscopy cannot tell about the inclination of the x,y axes in optically uniaxial phases, i.e. hexagonal and square, GISAXS experiments can. For discotic columnar phases

the densely packed {100} planes are shown by GISAXS to be parallel to the substrate in most cases.[95b,98] In hexagonal honeycombs the {100} planes are also most often parallel to the substrate, the hexagons thus standing on their apex.

The inclination of the reciprocal lattice observed by GISAXS often helps with structure determination, since the tilt must have a rationale in the proposed structure. An example is given in Figure 20, which shows the GISAXS patterns of the stretched hexagonal honeycombs in compounds **1e** and **1f** discussed in section 2.3. The models of the honeycombs in Figure 20c,d give a rational explanation of the different orientations observed in the diffraction patterns. [44,49]

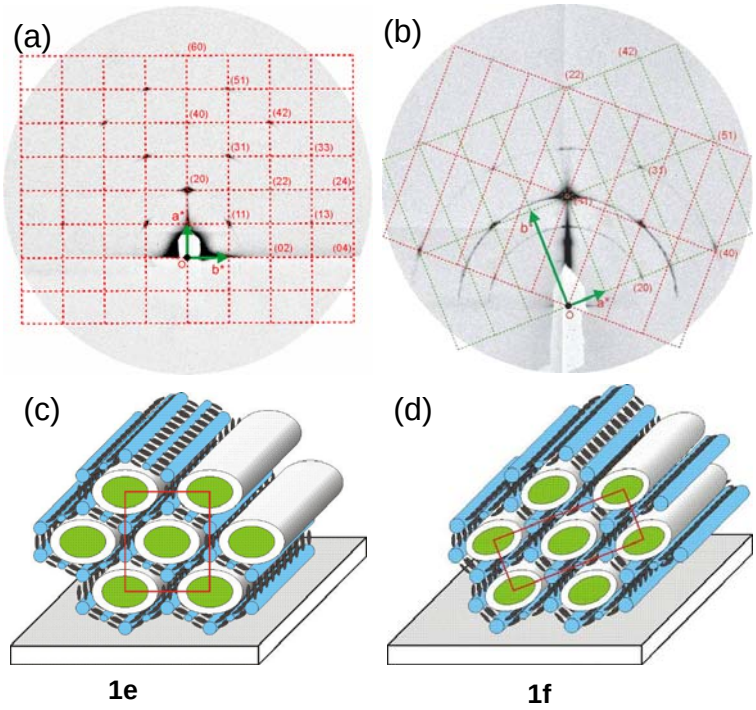

Figure 20. a,b) GISAXS patterns of rectangular columnar *c*2*mm* phases in a) compound **1e** at 60°C and b) compound **1f** at 115 °C – see Figure 8 for chemical structures; c,d) structures of the stretched hexagonal honeycomb phases resting on the substrate surface. [44,49] Reproduced with permission.[49] Copyright 2010, Institute of Physics.

6.2 Monolayers on solid surfaces

Thin organic films are of importance for numerous nanotechnological applications, such as superhydrophobic, antibacterial or command surfaces and for molecular electronic devices, to mention but a few. Beside spin coating, vapour deposition and spontaneous self assembly from solution, transfer of preformed monomolecular films onto surfaces (Langmuir-Blodgett films) represents another commonly used technique for preparation of thin films.[100] Therefore, T-shaped and X-shaped polyphiles were investigated with respect to formation of

defined structures at solid surface as well as in mono- and multilayers at the air water interface.

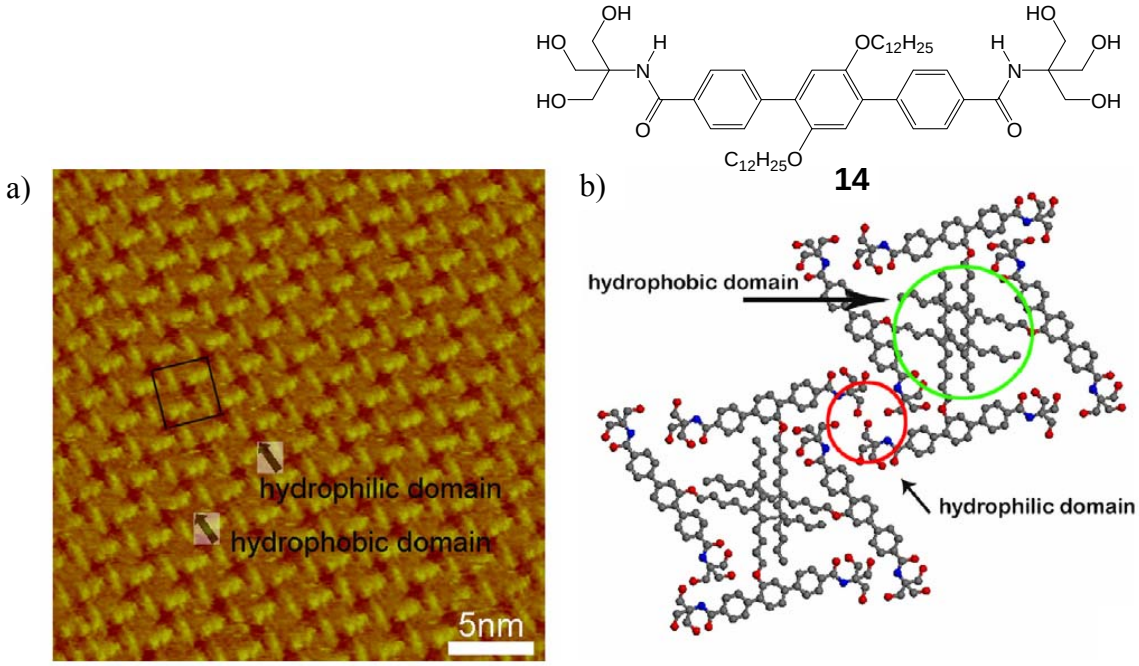

Figure 21. a) STM images of the well-ordered assembly of compound **14** on HOPG and b) the corresponding packing model, alkoxy groups on the periphery are omitted for simplicity. Reproduced with permission.[101] Copyright 2008, Elsevier.

To the best of our knowledge there is only one report about defined self assembly of X-shaped polyphilic molecules in monomolecular layers on solid surfaces. [101] In thin layers of compound **14** on HOPG a nearly square honeycomb motif is formed by the terphenyl cores with hydrophilic and hydrophobic parts segregated inside the cells and at the nodes, respectively (see Figure 21). However, there is a significant staggering of the aromatic cores, leading to a distortion of the square lattice and to a kind of herringbone-like pattern which might be due to the competition between the intrinsic self assembly of the polyphilic molecules on a square grid, driven by hydrogen bonding and space filling, and the forces provided by the interaction of the alkyl chains and the aromatic cores with the graphite surface.[101]

6.3 Organization on water surface and in Langmuir-Blodgett films

Polygonal honeycomb structures are completely lost if T-shaped and X-shaped polyphilic molecules are assembled at the air-water interface, as the interaction with the bulk water becomes the dominating organizing force in this case. Nevertheless, the Langmuir films

formed by these molecules show some remarkable, even unique properties. Usually, for simple amphiphiles composed only of a hydrophilic group and one or two alkyl chains, well defined Langmuir films of monomolecular thickness can be easily prepared. However, upon further compression of such films, disordered molecular aggregation takes place, making repeated compression/decompression runs irreversible.[102] In contrast, for several types of T-shaped and X-shaped polyphiles reversibility and the formation of well-defined multilayers was observed.

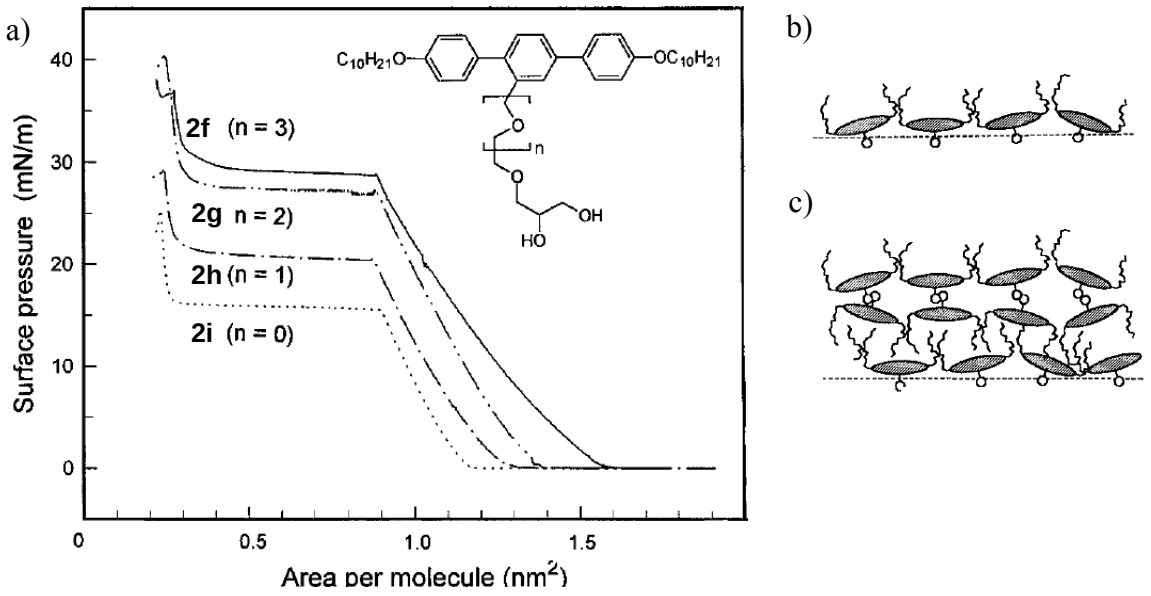

Figure 22. a) Surface pressure/molecular area isotherms of monolayers of compounds **2f-2i** at the air-water interface (T = 20 °C) and b,c) schematic presentation of the possible arrangements of these facial amphiphiles at the air-water interface: b) monolayer with a side-on arrangement of the molecules and c) well defined triple layer formed by the overlay of a bilayer on top of the monolayer. Reproduced with permission.[103a] Copyright 1997, American Chemical Society.

T-shaped facial amphiphiles (compounds **2f-2i)** represent typical examples of molecules forming such well-defined triple layers. Their Langmuir isotherms show a broad plateau which is reached at areas corresponding to the area required by the bolaamphiphilic core lying flat on the surface – see Figure 22.[103] The plateau ends and a second rise starts at an area per molecule corresponding to about one third of the molecular area. This suggests triple layer formation which sets in at the beginning of the plateau. It was assumed that the polar lateral groups interact strongly with the water surface causing these molecules to lie flat on the air/water interface creating stable Langmuir films. The terminal chains are likely to pack on top of the aromatic core. At the onset of the plateau the molecules are packed in a 2D film

with maximum density. On further compression (in the plateau region) the molecules are removed from the surface and "escaping into the third dimension" during formation of the triple layer.

The same type of isotherms was recently found for X-shaped bolaamphiphiles **5,** such as compound **5a** for example (see Figure 10).[104] These compounds with one or two short fluorinated segments show a complete reversibility and reproducibility of the isotherms in spite of the compression to complete collapse of the film and even for the highest possible compression/decompression rate of 1.50 nm^2/molecule/min. Three cycles for compound **5a** are shown in Figure 23a. The reversibility manifests itself as perfectly overlapping isotherms, $\pi(A)$, with the same surface pressure at the plateau observed in both directions. The Brewster angle microscopy (BAM) images in the plateau region show coexistence of two liquid phases of very different thickness (see Figure 23b-e). This is in line with the proposed formation of closely packed and well defined trilayers and also indicates the fluidity of these layers. However, only polyphiles with short fluorinated segments in the lateral chains give these perfectly reversible isotherms, whereas for related non-fluorinated compounds this process is irreversible.

High reversibility seems to be due to the liquid-crystalline character of the multilayer structures, which resemble the thermotropic lamellar phases found for some of the X-shaped bolaamphiphiles in the bulk.[23,25] The fluidity of these structures, which seems to be increased by partial fluorination of the side chains, prevents the monolayers from chaotic aggregation, improves the stability of the films at the air/water interface, and allows the formation of well-defined triple layers with perfection comparable to that of freely suspended films of smectic liquid crystals.[105]

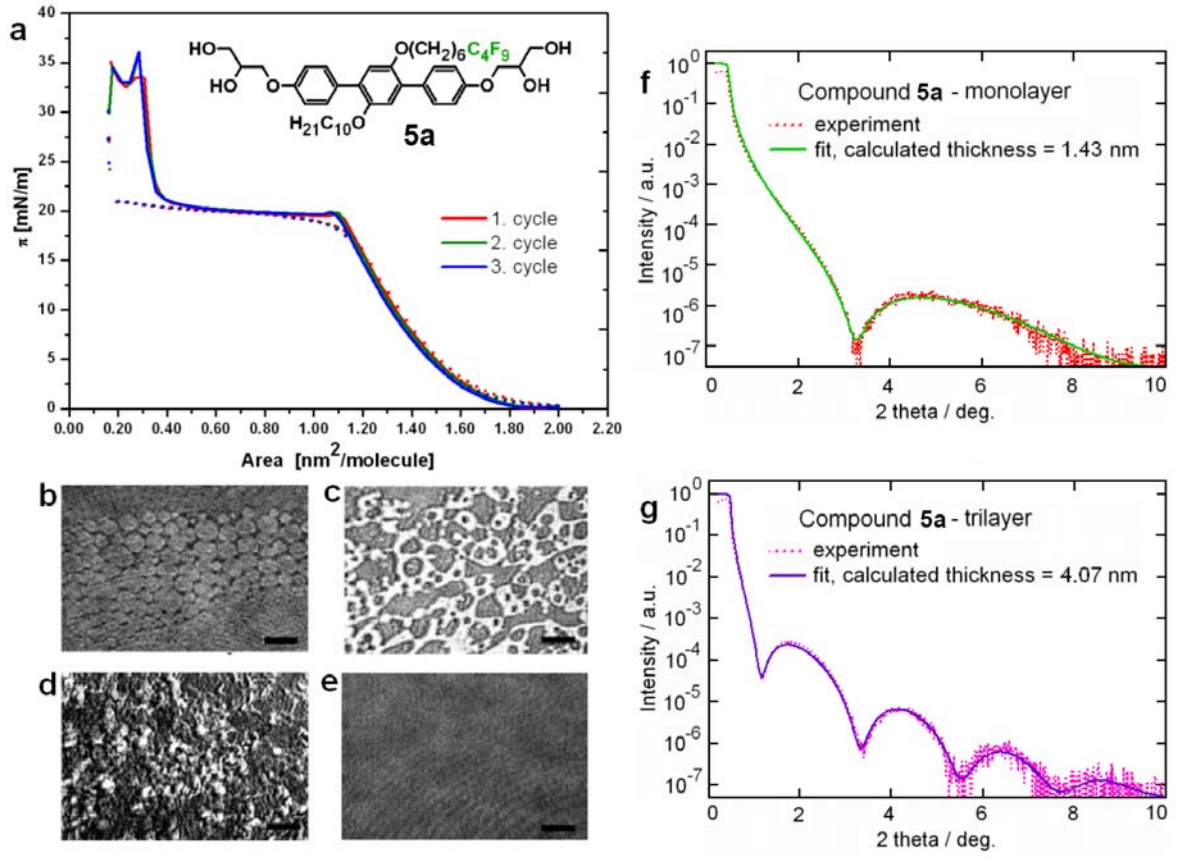

Figure 23. a) Reversible isotherm of compound **5a** (3 cycles) giving the same surface pressure at the plateau: solid and dotted lines correspond to compression and decompression runs, respectively; b-e) the BAM images show: b) coexistence of gas and expanded liquid (2D foam) before the plateau, c) coexistence of monolayer (darker areas) and trilayer (brighter areas) in the plateau region, d) aggregates after complete collapse, e) uniform film of the monolayer recovered during decompression, f,g) results of x-ray reflectivity from f) the monolayer and g) trilayer of compound **5a** transferred onto the silicon substrates at surface pressures 15 mN/m and 30 mN/m, respectively. Reproduced with permission.[104] Copyright 2010, Royal Society of Chemistry.

Formation of the trilayer structure was additionally verified by X-ray reflectivity of the films transferred onto the silicon substrates, as shown in Figure 23f, g as an example. The obtained reflectivity curves are very similar to those obtained for freely suspended liquid-crystalline smectic films,[105] indicating highly uniform layers. Experimental evidence was in agreement with mon- and trilayer nature of the films. Film uniformity is completely preserved during transfer to a solid substrate. This allows rapid transfer of three layers at a time in each dip.

Reversible formation of well-defined single-, triple and even thicker multilayers by compression of monolayers was also reported for amphiphilic liquid crystals with a polar group at only one end, and incorporating rod-like[106,107,108,109,110,111] or disc-like anisometric units.[112] For these compounds predominately vertical or tilted alignment of the rigid cores was observed, whereas bolaamphiphiles with polar groups at both ends adopt the side-on-

arrangement in monolayers.[113] This indicates that the proper combination of rigid rod-like and flexible units is a general approach to fluid, but well defined mono and multilayers. Moreover, depending on the molecular topology either SmA or SmC–like structures (aromatic cores perpendicular or tilted to the layer planes)[106,107,108,109] or structures similar to the Lam phase[25] where the aromatic cores are aligned parallel to the layers could be obtained. The former type is typical for linear rod-like amphiphiles without lateral chains, whereas the latter has become available with the T-shaped and X-shaped polyphiles.[104]

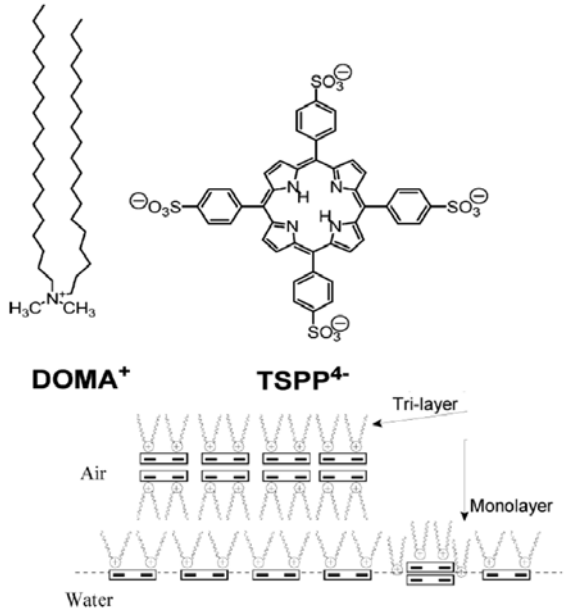

Figure 24. Model of the proposed organization of the mixed layers formed by coassembly of TSPP and DOMA at the air-water interface in the monolayer and trilayer structures. Reproduced with permission.[112] Copyright 2004, American Chemical Society.

Reversible trilayer formation at the air-water interface was also observed for amphiphiles with bulky aromatic end groups,[114] and for mixed monolayer containing a cationic lipid ($DOMA^+$) and an anionic porphyrin ($TSPP^{4-}$, see Figure 24).[112] Similarity to the self assembly of X-shaped bolaamphiphiles stems in this case from the fact that the interaction between cationic lipids and the anionic porphyrins (ionic self assembly) leads to supramolecular aggregates with polar groups at the end of (disc-like) aromatic cores which arrange parallel to the layers, while the layers themselves are separated by the vertically oriented flexible chains (Figure 24). In this case the reversibility was explained by line tension of the trilayer domains coexisting with residues of monolayer.[115]

Rod-coil molecules with facial amphiphilic topology (e.g. compounds related to **7e**, see Figure 13, but with two additional benzene rings in the rod-like core) also form stable monolayers with side-on organization of the rod-like aromatic cores. However, due to the absence of additional flexible alkyl chains the layers are more rigid and increasing the surface pressure leads in this case to a transition to vertical orientation of the aromatic cores and to the formation of (in some cases helical) fibres instead of defined triple layers.[116]

7 Polyphilic star polymers

While the systems discussed so far self-assemble into liquid-crystalline structures with unit-cell sizes in the range of very few nanometers, microphase separated block copolymers are known to self-assemble in regular structures on length scales between 10 to 100 nm. As there is much literatures available on the self-assembly of block copolymers in general, we just refer here to a few more recent review papers.[117,118,119] In the following section we will focus on results published on tailor-made branched polymers composed of more than two different components forming separate arms. These are mainly *3-miktoarm star terpolymers* (here also abbreviated as star-terpolymers), as up to now there are no reported experimental data on the morphology of star copolymers composed of more than three chemically different arms. Unlike linear triblock terpolymers (or linear block copolymers with more than three components), these branched polymers sometimes self-assemble into structures which are similar to the ones observed in the branched low-molecular weight liquid crystals discussed above. It must be said however that the degree of order in the "ordered" phases of block copolymers is usually considerably lower than that in LCs, with a few notable exceptions. In most cases the type of order can be described as paracrystalline.[120] This lack of true long-range order means that crystallography-based electron density reconstruction is rarely feasible in copolymers. Scattering method therefore normally has to rely on assumed models and form-factors. On the other hand the increased length-scale makes block copolymer morphology easier to observe with TEM.

Due to the low entropy of mixing of polymers, the chemically different arms of a star polymer will generally have a stronger tendency to phase separate than the small building blocks of polyphilic liquid crystals. Thus the choice of polymer blocks is considerably wider than that of the functional groups in LC amphiphiles. The first 3-miktoarm star terpolymer forming distinct microdomains of all three components was reported by Fujimoto et al.[121] and later on its morphology was discussed by Okamoto et al.[122] They described a system composed of three rather strongly incompatible components, namely polystyrene, poly(*t*-butyl

methacrylate) and polydimethylsiloxane. They stated a cocontinuous arrangement of all three components. However, the transmission electron micrographs and the schematics also indicate a two dimensional projection of a trigonal morphology consisting of 3 hexagon-like microdomains such as (6^3) in Figure 1.

More studies were carried out by Hadjichristidis group on 3-miktoarm star terpolymers formed by polystyrene (S), polyisoprene (I) and poly(methyl methacrylate) (M). They reported a hexagonally packed core-shell cylindrical morphology with a constant mean curvature (Figure 25a) and a periodic core-shell morphology with rectangular *c*2*mm* symmetry composed of rhombic cylinders (Figure 25), which was explained by the competing influences of chain stretching and minimising the interfacial area.[123]

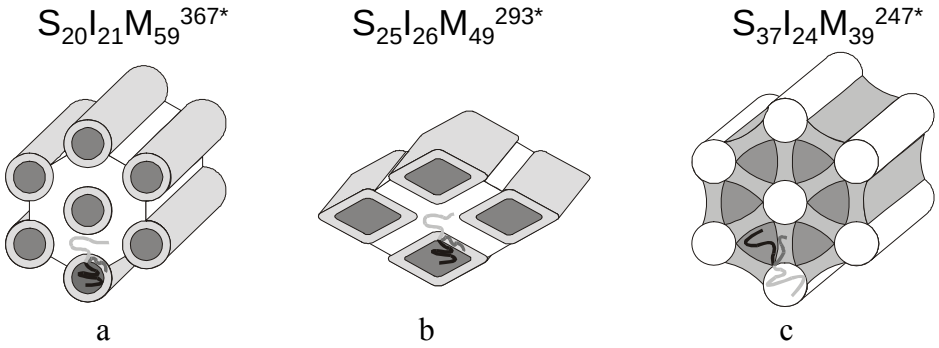

Figure 25. Schematics of the morphologies formed by polystyrene-*arm*-polyisoprene-*arm*-poly(methyl methacrylate) miktoarm star terpolymers. Lower case numbers indicate the weight percentage, upper case number is the molecular weight in kg/mol, * indicates the star topology. Dark-grey: polyisoprene (I), light-grey: polystyrene (S), white: poly(methyl methacrylate) (M). Note the analogy with T-shape amphiphile structures with hexagonal, rhombic and triangular cylinders, respectively, in Figure 1f, Figure **2**e and Figure 1c. Reproduced with permission. [134] Copyright 2003, John Wiley & Sons).

It is worth noting that in this system the junction points between the three different arms seem to be located within the polystyrene shell, which separates the poly(methyl methacrylate) matrix from the polyisoprene core cylinders, since these two components have the strongest incompatibility in this system. Later they reported on the same system with a lower amount of poly(methyl methacrylate) a structure evidencing the localisation of the junction points along lines rather than being dispersed in one of the microdomains.[124] This structure shows 6-fold symmetry and also has interfaces between the microdomains with non-constant mean curvatures (Figure 25c). Surprisingly, the same morphology was found for a linear triblock terpolymer before, namely polystyrene-*block*-poly((4-vinylbenzyl)dimethylamine)-*block*-polyisoprene, when cast from a selective solvent.[125] The same triblock terpolymer showed a

lamellar morphology when cast from a less selective solvent. This indicates that kinetic effects may also lead to non-constant mean curvatures in linear block copolymers, which could self-assemble in structures with constant mean curvature when at equilibrium.

Viewing polystyrene as the aromatic moiety, the polyisoprene arm as the aliphatic chain and poly(methylmethacrylate as the polar group, this structure with 6-fold symmetry (Figure 25c) consists of triangular cylinders with aromatic cylinder walls, fused by the polar groups at the edges and the cylinder cells filled by the aliphatic chains. With respect to the cylinder shape and the distribution of the different material components this is fundamentally the same structure as recently reported for the triangular cylinder phase formed by X-shaped bolaamphiphiles with two lateral alkyl chains (compound **1c**, $n = m = 6$, Figure 5)[34] but on a much larger length scale.

A major difference in the molecular topology between the X-and T-shaped polyphiles and the star terpolymers is the nature of the linking of the chains. In the case of star terpolymers of three strongly incompatible components with rather similar volume fractions this is at a point, lining up to a line in the polymer morphology and at this line all three different cells meet (Figure 26a). In the X and T-shaped amphiphiles this junction point is extended to a junction line and this line represents an incompatible segment of its own which is rigid and forms the cylinder walls of the polygonal honeycombs (Figure 26b, c).

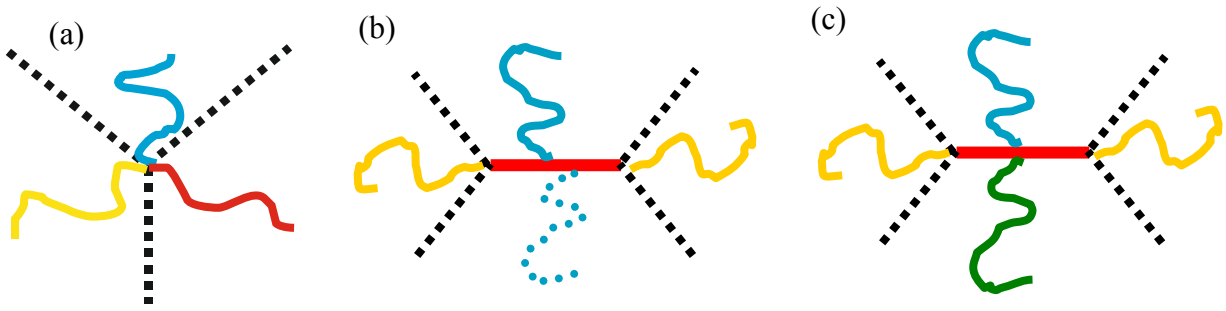

Figure 26. a) 3-Miktoarm star terpolymer, b) T-shaped or X-shaped ternary block molecule, c) X-shaped quaternary block molecule.

Hadjichristidis group synthesized later on a polystyrene-*arm*-polyisoprene-*arm*-poly(dimethyl siloxane) 3-miktoarm star terpolymer, which was shown to have a square symmetry by TEM tomography.[126] Blends of this polymer with polydimethylsiloxane showed the same square symmetry and an excess of PDMS homopolymer was excluded from the superstructure rather than having altered the morphology of the ordered phase. The addition of polystyrene lead to a 2D hexagonal structure and further addition of polystyrene reduced the degree of order.[127]

Hückstädt et al. introduced 3-miktoarm star terpolymers based on polystyrene, poly(1,2-butadiene) and poly(methyl methacrylate).[128] Later on they worked on polystyrene, poly(2-vinylpyridine), and poly(1,2-butadiene)[129,130] or polyisoprene[131] as the most flexible component. In all these systems they used a coupling strategy different from the ones introduced before. This coupling strategy was then further developed by others, especially Hirao's group could increase the number of different arms dramatically, up to seven.[132] However, from these systems no morphological characterisations were published so far. A polystyrene-*arm*-polyisprene-*arm*-poly(γ-benzyl-L-glutamate) 3-miktoarm star terpolymer showed a wavy morphology which was interpreted as polyisoprene cylinders in a matrix of the polyamide.[133] The systems published by Hückstädt et al. are based on three different polystyrene-*block*-polybutadiene diblock copolymers of cylindrical, lamellar, and inverse cylindrical composition. These diblock copolymers had an initiating function at the junction point and various amounts of 2-vinylpyridine were polymerised from that junction point, leading to three sets of star terpolymers with varying amounts of poly(2-vinylpyridine). The characterisation of the morphologies of these polymers by TEM is facilitated by the combination of various staining techniques highlighting selectively different components of the star terpolymer. Besides the fact, that all three components are rather strongly immiscible with each other, this applicability of different staining techniques was a major advantage compared to other systems. A schematic summary of the morphologies found is given in Figure 27.[134]

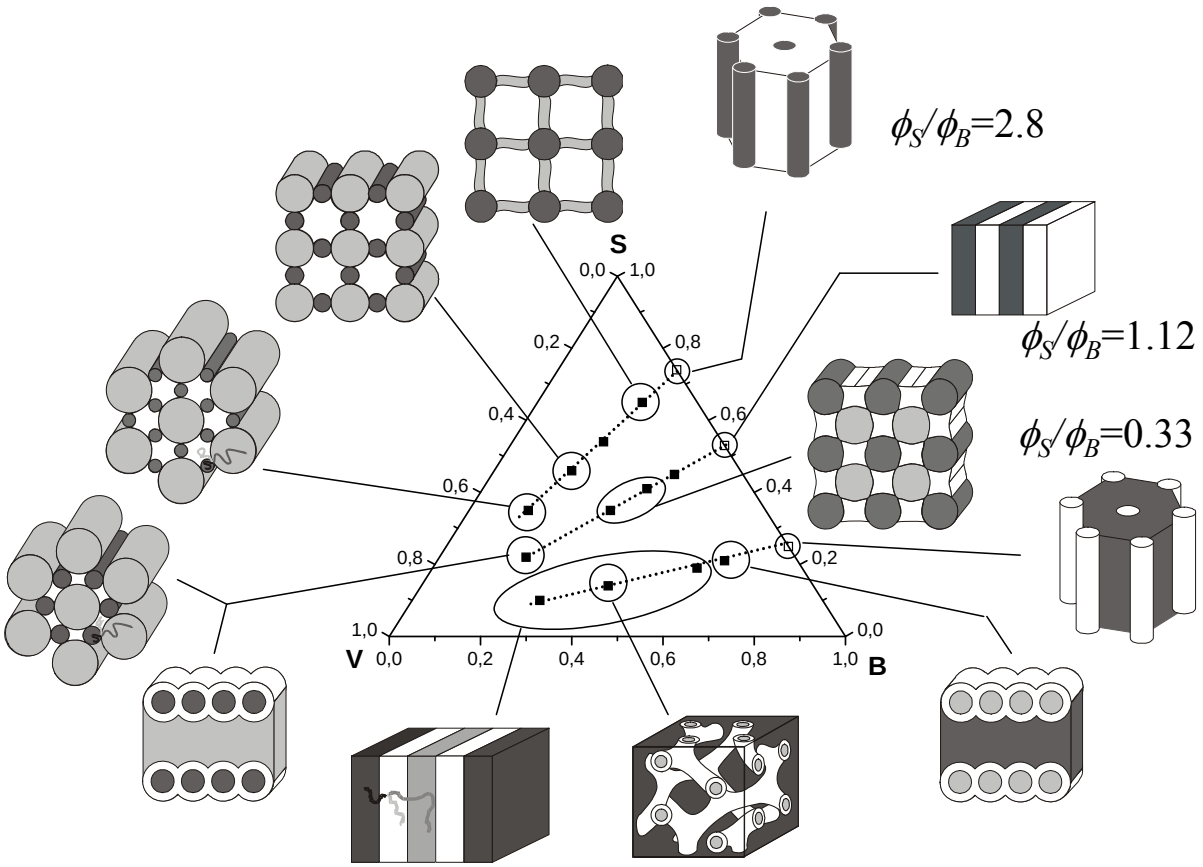

Figure 27. Schematics of the morphologies formed by polystyrene-*arm*-polyibutadiene-*arm*-poly(2-vinyl pyridine) miktoarm star terpolymers. Dark: polybutadiene (B), grey: poly(2-vinyl pyridine) (V), bright: polystyrene (S). The compositional ratios 2.8, 1.12, and 0.33 correspond to the SB-precursor diblock copolymers carrying the initiating group for V-polymerisation at the junction point. Reproduced with permission.[134] Copyright 2003, John Wiley & Sons).

Again the square and hexagonal morphologies of the star terpolymers have analogues in square and hexagonal cylinder phases of low molecular mass T- and X-shaped polyphiles. Also similar to the X-shaped and T-shaped polyphiles the polymer morphology mainly depends on the volume fractions of the incompatible segments. In the case of the polymeric systems, the conformational entropy of the arms is of much more importance compared to the low molecular weight LC's. Some systematic morphological relationships among these structures were highlighted before,[134] and as an example in Figure 28 some of these are shown. The figure illustrated how symmetry positions between two components are exchanged, and how a square morphology converts to hexagonal as the volume fraction of the largest component increases. A similar exchange between two hexagonal morphologies (right column of Figure 28) could also be achieved by blending with a symmetric diblock copolymer, which is miscible with the two larger arms of the star terpolymer.[135] This is shown in Figure 29, where the addition of a polystyrene-*block*-poly(2-vinylpyridine) diblock

copolymer leads to an exchange in positions between polystyrene and poly(1,2-butadiene). While a homopolymer in a blend with a miktoarm star terpolymer can be localised almost anywhere in the respective compatible microdomain, a diblock copolymer in such a blend will localize at the 2D interface between the two microdomains, which are compatible with the two blocks of the diblock copolymer, respectively.

Again, considering the polystyrene as the aromatic unit, the polybutadiene arm as the aliphatic chain and the poly(methyl methacrylate) as the polar group, the two hexagonal phases shown in Figure 29a and b can be related to the hexagonal honeycomb LC phases of the anchor-shaped polyphile **3b** (Figure 7b) having the aromatics at the nodes and the polar groups in the middle of the walls and T-shaped bolaamphiphiles of type **1** (Figure 7a) having the aromatics in the cylinder walls and the polar groups at the nodes, respectively.

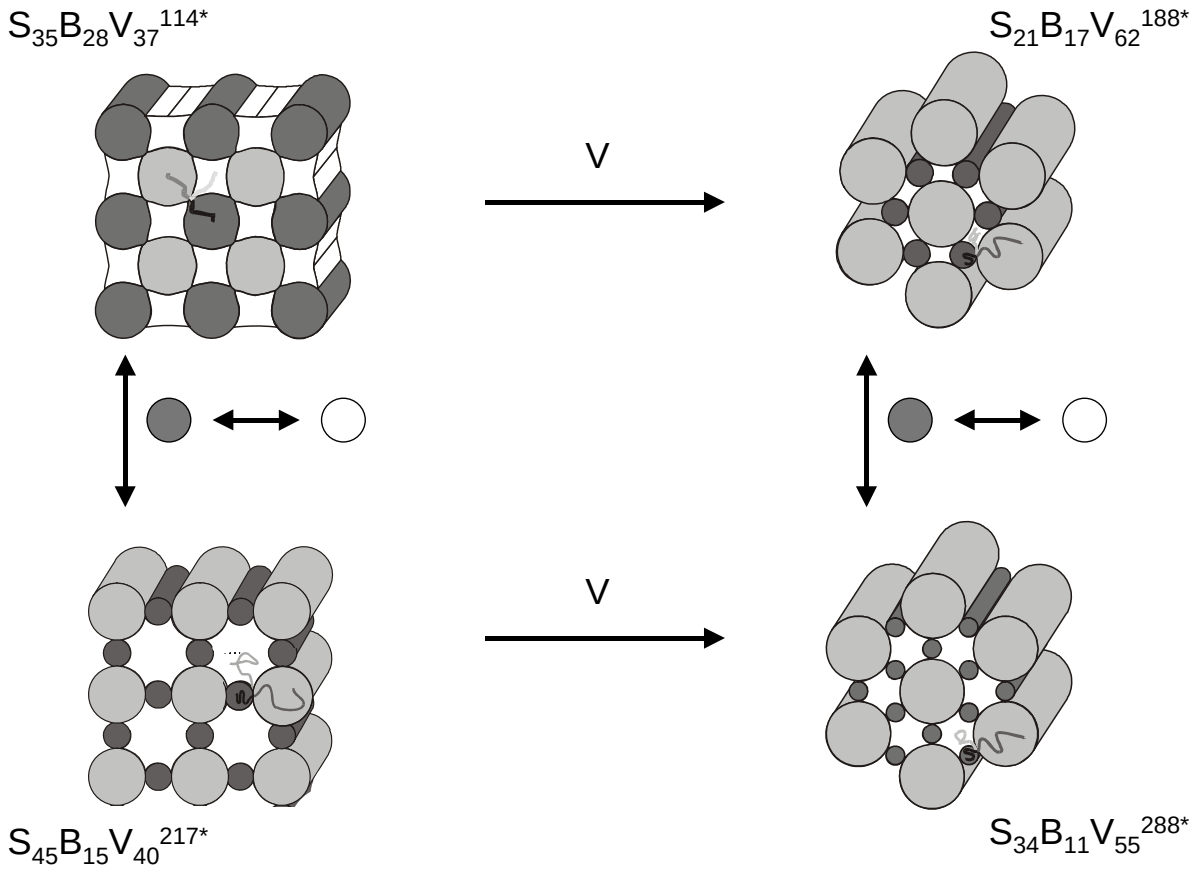

Figure 28. Schematics of the morphologies formed by polystyrene-*arm*-polybutadiene-*arm*-poly(2-vinyl pyridine) miktoarm star terpolymers. Black: polybutadiene (B), grey: poly(2-vinyl pyridine) V), white: polystyrene (S). Number codes as in Figure 25. Reproduced with permission.[134] Copyright 2003, John Wiley & Sons).

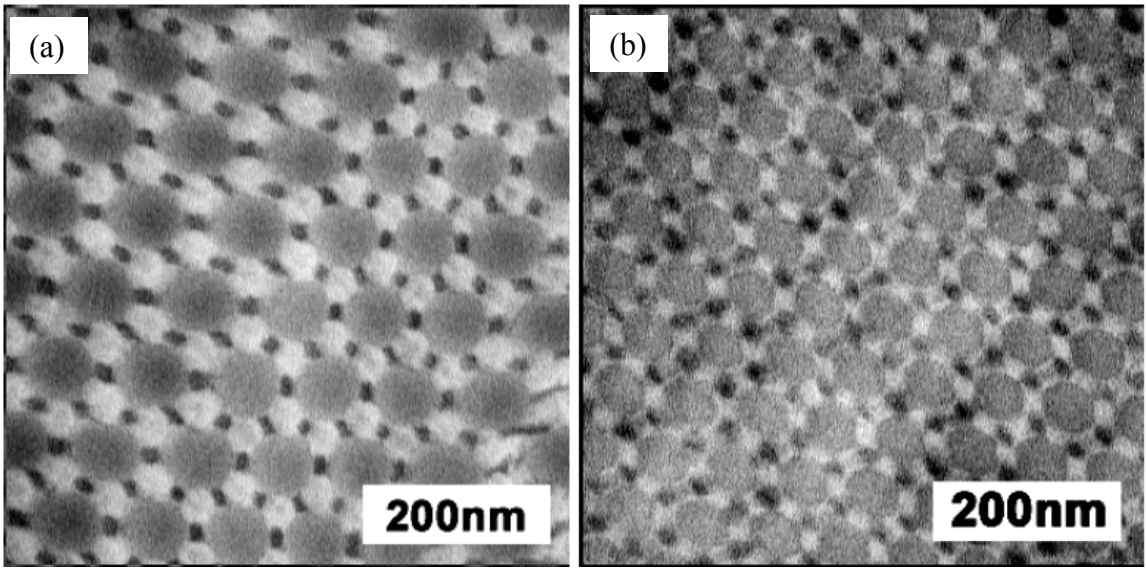

Figure 29. a) TEM of $S_{34}B_{11}V_{55}^{288*}$ and b) a blend of $S_{34}B_{11}V_{55}^{288*}$ and $S_{45}V_{55}^{76}$ diblock copolymer (1:1 by weight). Number codes as in Figure 25, color code as in Figure 28. Reproduced with permission [135]. Copyright 2004, European Polymer Federation.

The SIM* systems shown in Figure 25a and b, also display core-shell type of morphologies as well as a lamellar morphology, as shown schematically at the bottom of Figure 27. In these cases the polystyrene microdomain separates the poly(1,2-butadiene) domains from the poly(2-vinylpyridine) domains completely, which forces some segments of these two latter components to be mixed within the polystyrene separating layers. For the lamellar structure it has been also confirmed theoretically that such a conformation in a 3-miktoarm star terpolymer composed of a rather non-selective arm (here polystyrene) and two strongly incompatible arms (here: polybutadiene, poly(2-vinylpyridine), or polyisoprene, poly(methyl methacrylate) may be favorable.[136]

Matsushita's group has worked in a systematic way on a similar system, where poly(1,2-butadiene) was replaced by polyisoprene.[137] They published a series of papers and discussed the morphologies in terms of Archimedean tilings, where applicable.[138] There are significant similarities with the tiling patterns in T- and X-shaped amphiphiles.

The tiling with *p*4*gm* symmetry (or reduced to *p*2*gg* symmetry or lower if distorted), shown in Figure 30[140] can be considered as a (3.3.4.3.4), or abbreviated (3^2.4.3.4) Archimedean tiling composed of triangles and squares with a ratio of 2:1 (dark lines in Figure 30a). The notation refers to the number of sides in successive polygons sharing the same vertex.[2b] We note the similarity with the simpler *p*4*gm* tiling of amphiphiles type **1** and **2** – see Figure 2f, Figure 3a and Figure 4b, where all the nodes are also of the (3^2.4.3.4) type. The (3^2.4.3.4)

tiling types are ubiquitous, both in 2D lattices and in lattice planes of 3D structures, both in soft matter [53,145] and in metals.[139] In fact a tiling identical to that in Figure 30 has been observed in LC honeycombs formed by T-shaped and X-shaped bolaamphiphiles (to be published). However, the morphology in Figure 30 can also be regarded as tiling of pentagonal cylinders (white line in Figure 30a), similar to the pentagonal cylinder phase of T-shaped facial amphiphiles **2** (aromatic units form the cylinder walls, aliphatic chains are located at the vertices and polar groups fill the cylinder cells) providing an example of topological duality in star terpolymer morphologies.[24,27] Similarly, the hexagonal morphology comprising triangular cells, shown in Figure 25c, can be regarded as the topological dual of the hexagonal morphologies with hexagonal cells as for example shown in Figure 29a.

The most spectacular structures found beside the ones showing Archimedean tiling patterns is a quasi crystal with a dodecagonal symmetry consisting of squares and triangles in a ratio different from 1:2, close to 1: 2.309.[140] The structure is a 2D equivalent of the dodecagonal liquid quasicrystal observed in a number of dendrimers systems.[141] Also a system showing the same cubic symmetry as zincblende was found, when a short homopolystyrene was added to a 3-miktoarm star terpolymer (Figure 31).[142] This shows that, as in the T-shaped LC polyphiles, beside 1D or 2D ordered structures, morphologies with a 3D lattice can also be achieved. These do not belong to the bicontinuous type, but can be considered as composed of discrete spherical aggregates. Hence they are related to the micellar cubic phases[143,144] and other 3D phases composed of spherical aggregates, such as the tetragonal[145] and the dodecagonal quasicrystalline phase[141] known from taper shaped amphiphiles[143] and dendrimers.[53,54,143] Notably, in these micellar cubic LC phases, even though the shape and size of the sphere-like aggregates can vary slightly, all spheres contain the same material. By contrast, in the star terpolymers the composition of the different spheres varies too, leading to a three-color 3D structure having two different types of micelles embedded in the continuum of the third (majority) component.

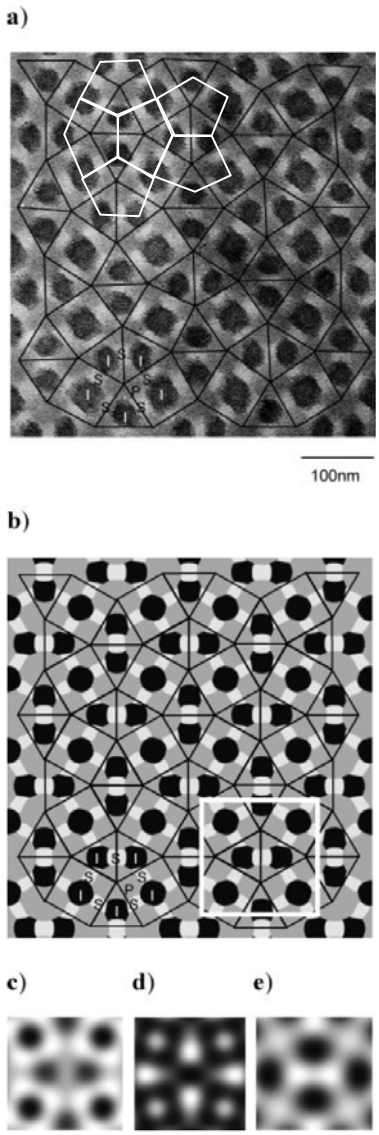

Figure 30. Comparison of domain packing manner between experimental (a) and calculated pattern (b). One of the Archimedean tiling patterns, (3^2.4.3.4), is drawn as thin solid lines throughout in (a) and (b); the dual Laves tiling is shown in white in (a). Parts (c), (d) and (e) represent density waves for I, S, and P phases, respectively, while (b) is drawn by summing them. Reproduced with permission.[140] Copyright 2005, John Wiley & Sons.

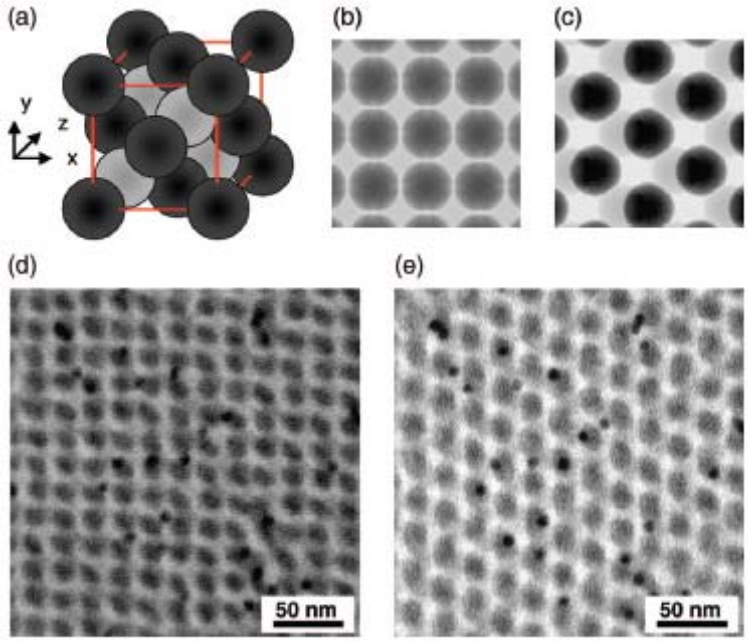

Figure 31. Schematic (a), simulations (b,c), and TEM (d,e) of the Zinkblende morphology formed by a polystyrene-*arm*-polyisoprene-*arm*-poly(2-vinyl pyridine) miktoarm star terpolymer. Dark: polyisoprene (I), grey: poly(2-vinyl pyridine) V), bright: polystyrene (S). Reproduced with permission.[142] Copyright 2008, American Chemical Society.

While all three arms in the star polymers described above are flexible, arms with longer persistence length can be introduced, such as polypeptides, particularly those forming an internally hydrogen-bonded α-helix. Introduction of a rigid arm presents a counterpart to the extensively studies rod-coil linear copolymers – see top of section 4. A star terpolymer composed of two coil-like arms (polystyrene, PS, and polyisoprene, PI) and a mesogenic α-helical polypeptide arm (poly(ε-tert-butyloxycarbonyl-**L**-lysine), PBLL) has been shown to form an ordered structure made up of alternating layers (Figure 32).[146] One of the layers comprises reasonably regular array of parallel PBLL helices standing normal to the layer surface, while the other layer consists of regularly alternating stripes of PS and PI. This phase may be compared to the Lam_{Sm} phase observed in some T-shaped bolaamphiphiles (Figure 1i), except that in the latter case the rigid rods are parallel to the layer surface and form one of the stripes.

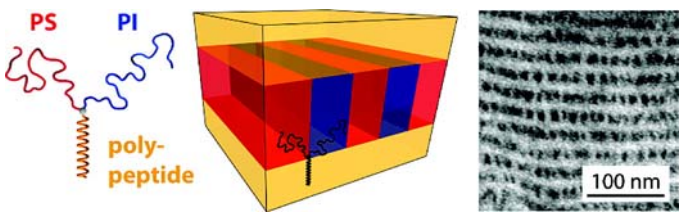

Figure 32. Ordered phase of a rod-coil star terpolymer, the three arms being polystyrene, polyisoprene and poly(ε-tert-butyloxycarbonyl-L-lysine). A schematic of the structure is shown in the center and a transmission electron micrograph of a stained section on the right (black is isoprene). Reproduced with permission.[146] Copyright 2010, American Chemical Society.

8 Computer simulations

Computer simulation[147] has become a very useful tool for understanding the structure of self-organised molecular systems. Since the length scales over which these systems self-organise are relatively large compared to the size of the molecules, it is necessary to use coarse grained models in which the chemical realism is somewhat sacrificed in favor of computational tractability. With a finite amount of computer time, we can typically study one molecule in significant detail and compare the results with experiment to see if they agree, or we can study many types or classes of molecules and compare general trends of how the behaviour varies as changes in the molecule are made. Thus instead of answering specific chemical questions about the molecules, we are typically more interested in answering more general questions about trends as specific molecular details are varied. For example, for the bolaamphiphiles already discussed, we can vary the length of a lateral chain whilst keeping the core and terminal polar groups of the molecule fixed.

Simulations have played an important role in understanding the behaviour of liquid crystals and polymers. For low molar mass liquid crystals, molecular or single site models such as the Gay-Berne potential[148] have been popular. For this model, a typical rod-shaped liquid crystal molecule is taken to be a rigid elongated site, with anisotropic attractive and repulsive interactions similar to the well-known Lennard-Jones potential. Simulations using this model have provided an understanding, at the molecular level, of the structure of nematic and smectic phases,[149] translational[150] and rotational[151] dynamics in the liquid crystalline phases, as well as being used to test assumptions in theories used to interpret X-ray[152] and other experimental data.[153] In contrast to the size and rigidity of liquid crystalline molecules, polymers tend to be significantly longer and more flexible. Thus simulation models developed for polymers focus on these molecular features. Many different approaches have been used to simulate polymers, from simple and self-avoiding random walks on lattices to atomic detail simulations, with many different levels of coarse-graining the realism of the model in between. Similarly, a range of simulation methodologies have been used, depending on whether we require an understanding of just the structure or also on the dynamics in the system. One model cannot possibly cover all length and time scales. An excellent review is given by Baschnagel et al.[154] When considering the molecular scale, polymers can typically

be modelled with a "chain of beads" model,[155] in which beads representing a number of atoms in the backbone of the polymer are bonded together with either a fixed or variable length bond. Interactions between the beads can be tailored depending on the polymer, solvent, and so on. The rigidity of the polymer can be easily modified by using bond angle potentials, or by setting limits on the distances between next-nearest neighbours in the chain. As well as simple homopolymers, such models are easily extendable to block copolymers by allowing for two (or more) types of bead with different interactions and to star and branched chain polymers by allowing three (or more) beads to be bonded at the branching sites.

To describe T- and X-shaped bolaamphiphiles, it seems sensible to develop models based on both liquid crystals and polymers with which they share common features. The formation of self-assembled structures in bolaamphiphiles and other soft matter systems typically occur over relatively large length and time scales, thus the use of a model based on the soft-core potentials used in dissipative particle dynamics[156] is appropriate. The DPD technique has been applied successfully to understand the structure and dynamics in simple block copolymers[157] of different length immiscible blocks. For example, the phase behaviour can be probed by simulations when the internal composition of the block-copolymer is varied. Such results can be compared both with experimental and theoretical (mean field) results to aid the understanding of the types of phases possible in block copolymer systems. More recently, a similar model has been used for rod-coil polymers,[158] where one region of the chain is flexible, the other completely rigid. These are shown to form only lamellar (smectic) phases, with the nematic phase common of many liquid crystals absent. Extensions of the di-block model to more components is trivial. Thus simulations of both linear and star tri-block models[159] have been performed to examine, for example, the shape morphology of vesicles forming in these systems in aqueous solutions as a function of the size of the different components, and the relative strength of the repulsive interactions.

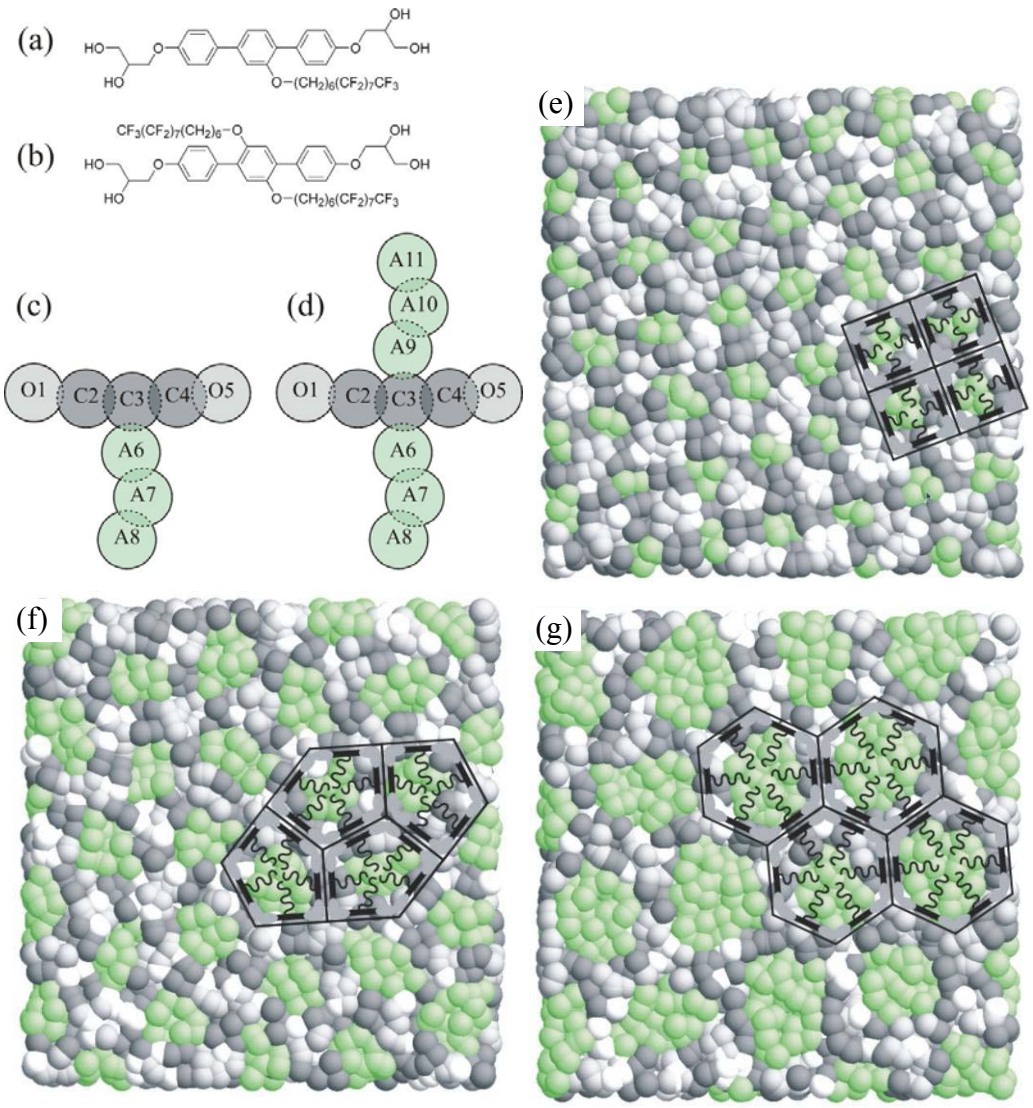

Figure 33. (a,c) T and (b,d) X-shaped bolaamphiphiles based on a *p*-terphenyl core with coarse grained representations suitable for dissipative particle dynamics simulations. Simulations of (e) the square, (f) pentagonal and (g) hexagonal columnar phases in T-shaped bolaamphiphiles. Color key: aromatic cores – grey, hydrophilic groups – white and lateral alkyl chain – green. Unit cells have been overlaid to indicate the locations of the cores and lateral chains. Reproduced with permission.[160] Copyright 2009, Royal Society of Chemistry.

Bates and Walker have developed a DPD model for bolaamphiphiles[160] based on a semi-rigid aromatic core with terminal hydrophilic groups and flexible lateral chains; multiple types of lateral chains are possible by varying the relative repulsive interactions between them.[161] Of course, when developing coarse grained models for such molecules many approaches are feasible, so long as the underlying physics of the model is correct. A similar approach using hard-body models has simultaneously been applied by Müller et al. to

understand T-shaped bolaamphiphiles in the bulk[162] and in aqueous solvents[163] based on soft repulsive models using molecular dynamics.

Computer simulations using these model potentials can be used to understand a number of different aspects of the formation of the columnar phases of T-shaped and X-shaped bolaamphiphiles. Perhaps the simplest example is the variation in the length of the lateral chain for a fixed core to reproduce the typical experimental phase diagram (see Figure 1 and Figure 2). Square, pentagonal and hexagonal columnar phases are all found[160,164] (see Figure 33) in simulations as the chain length is increased, as well as columns with extended hexagonal cross sections and lamellar phases for even longer chains. A similar range of columnar phases are observed using a fully rigid central core.[162]

Within the soft repulsive model used with the dissipative particle dynamics thermostat, the molecule of interest is broken into different parts, then each part is broken into smaller parts of similar size (see Figure 33c,d). These units, composed of typically 6-10 carbon or similar atoms, are represented by a single bead. These beads are linked together using a harmonic spring such that the topology of the model molecule is the same as that of the real molecule; full details are given in the original paper.[160] Building the model molecule in this way is particularly flexible; it is trivial to vary the length of the core, the lateral chain lengths, the position of the lateral chain, and so on. Similarly, it is simple to vary the relative miscibility of the lateral chains when there is more than one chain by varying the relative repulsive parameters. The chemical detail may appear lost. However, as well as the molecular topology and the coarse grained interactions between the beads, some chemical realism can be built in at larger length scales. For example, one bead in the chain can be parameterised as an alkyl chain, and the rest as fluorinated chain, to represent the alkyl spacer commonly used to attach fluorinated chains to the aromatic core.

Once these phases have been identified in simulations, we can start to understand structural properties. For example, it is clear that squares and (regular) hexagons tile 2D space, whilst (regular) pentagons cannot. The structure of the pentagonal columnar phase can be examined in the simulation to understand how pentagonal columns can form. Simulations indicate that the perimeter of the pentagonal columns retain their integer number of rod-like cores as expected, with the hydrophilic groups at the vertices. However, the angles formed at the vertices,[164] which are easy to determine for a simulation model, indicate that the pentagons formed are not regular (cf. also Figure 3a, Figure 4c and Figure 6[24]). The distribution of angles at the vertices for the pentagonal phase deviate from 72°. In contrast, the angles

formed at the vertices between the rod-like cores for the square columnar phase are peaked strongly around 90° and 180°, and for the hexagonal columnar at 120°, as we expect for regular square and hexagonal tiling.

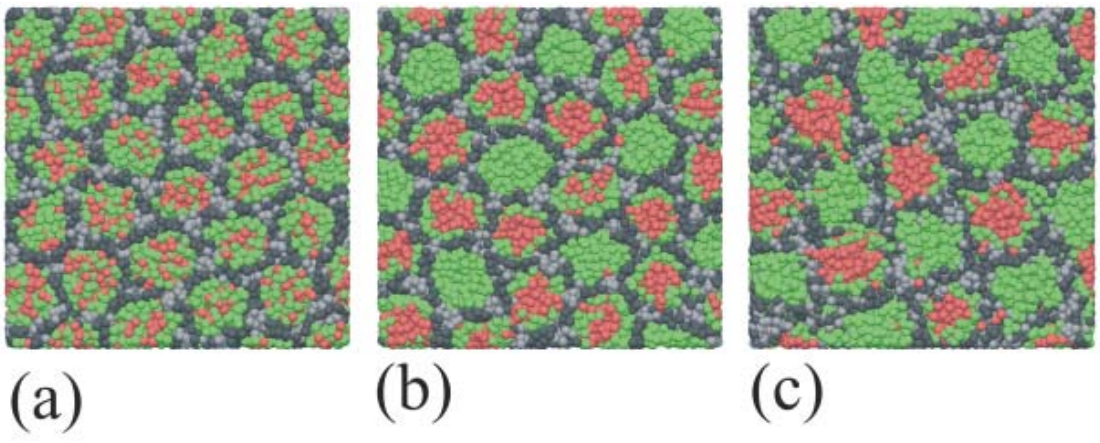

Figure 34. Snapshots for chains with an alkyl spacer. (a) When the different chains are miscible, then a hexagonal columnar phase is observed. (b) As the miscibility of the chains is decreased, a new demixed hexagonal columnar phase is observed. (c) As the miscibility parameter is reduced further, the hexagonal columnar phases are destabilised with respect to the demixed square columnar phase. All three phases have recently been observed experimentally – for those in (a) and (b) see ref.[57]. Reproduced with permission. [161] Copyright 2009, Royal Society of Chemistry.

Simulations, even of coarse grained models, can also be used to predict phases that should be observed when the molecular features are varied. One example is what should happen when an X-shaped bolaamphiphile has immiscible lateral chains, the topic discussed in section 3.2. If the length of the chains is such that the bolaamphiphile would normally form a square columnar phase when the chains mix, then simulations predict that a square columnar phase should also form for the chains which tend to demix. Note that this reduces to a coloring problem; since each molecular core has a different type of chain on each side, each tile has to be colored such that a different color occurs where the edges of tiles touch. For square tiling, it is clear that the 2D plane can be colored with only two colors in this way. In contrast, hexagonal tiles cannot be colored with only two colors and so we expect frustration. Simulations have shown that if the two lateral chains are fully hydrogenated on one side, and fully fluorinated on the other, then the hexagonal columnar phase is destabilised completely. This can be easily seen in Figure 34, where green is used to represent the alkyl regions of the chains and red the fluorinated. Even when the lengths of the chains are chosen such that the

hexagonal columnar phase should occur, the frustration leads to a square columnar phase.[161] However, a different situation can be observed when the lateral chain is not fully fluorinated. If an alkyl spacer is used to attach a fluorinated chain to the molecular core (as is actually the case for nearly all reported T- and X-shaped polyphiles), then a hexagonal columnar phase can be observed. When demixing of the lateral chains occurs for a hexagonal columnar phase, one pure column is formed, containing only alkyl chains. A second type of column is formed which necessarily contains a mixture of fluorinated and alkyl chains. Thus the frustration of the molecule that is located on the boundary of two fluorinated columns can be relieved by the familiar core-shell local separation of alkyl and fluoroalkyl segments (Figure 34b, compare with Figure 7 and Figure 8). This explains why a hexagonal columnar phase can be observed if the fluorinated chain is attached with an alkyl spacer. Both the "core-shell" mixed hexagonal phase and the two-color superlattice phase in Figure 34a and Figure 34b have actually been observed experimentally,[57] inspiring the simulation of multicolor honeycombs.

Finally, if two different length miscible chains are used, then they appear to act, to a first approximation, as the average of the two. For example, short (2 bead) chains form a square columnar phase, medium (3 bead) chains form a hexagonal columnar phase and longer (4-5 bead) chains form a lamellar phase. For a model bolaamphiphile with one short and one longer chain, then a hexagonal columnar phase is observed.[161] In contrast, when immiscible chains of different lengths are used, then this opens up the possibility of multiple column types and shapes, as already discussed in section 3.2. This is realised most readily in the kagome columnar liquid crystal phase of hexagons and triangles[55] (see Figure 11d). Incidentally, note that the difference between the atomistic simulation in Figure 11c and the coarse grain simulation in Figure 11d is that in the former an approximate model had been built beforehand and then allowed to anneal through molecular dynamics of one unit cell with periodic boundaries, primarily to confirm that the structure suggested by geometry considerations and electron density map is viable with regard to space filling. In contrast, the arrangement in Figure 11d arose spontaneously from a random liquid through DPD simulation of a large system.

Crane and Müller have used their rigid core model to examine the swelling of the columnar phases when the T-shaped bolaamphiphile is mixed with a solvent, with interactions similar to those of benzene. In particular, they vary the amount of solvent and examine the effect on the hexagonal columnar phase. For very small amounts of solvent, the hexagonal columnar phase remains stable, with the extra solvent incorporated into the columnar phase. However, when the solvent concentration is greater than about 5%, the system splits into two distinct phases,

one rich in bolaamphiphile, the other rich in solvent (see Figure 35). The two phase separation is observed down to low concentrations of the bolaamphiphile, although above about 70% solvent concentration, the hexagonal columnar nature of the bolaamphiphile rich region is lost. Such simulations should help explain some of the existing[178] and future experimental data on binary systems T-shaped amphiphile – solvent.

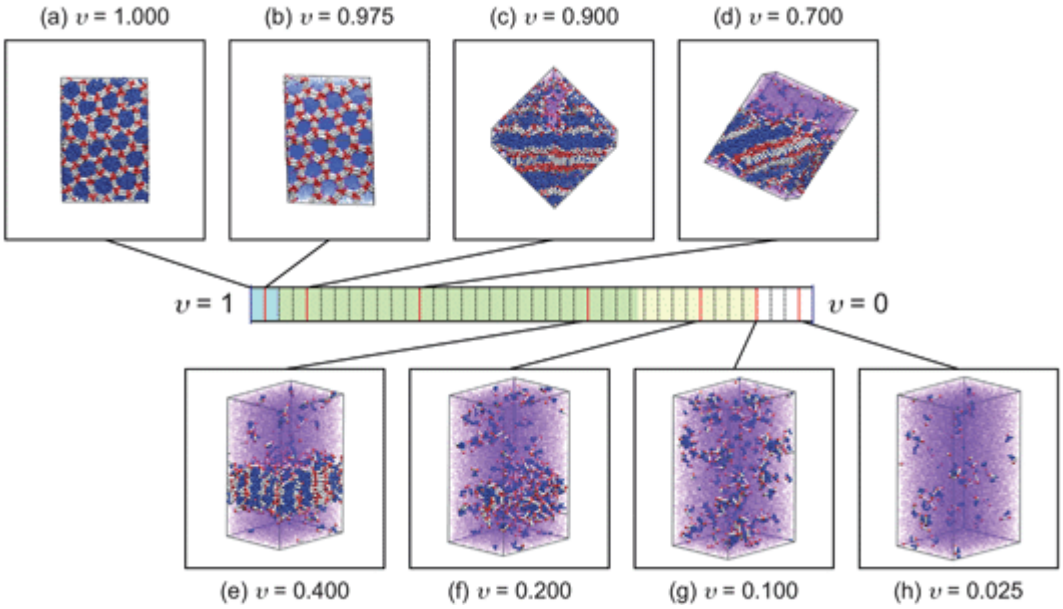

Figure 35. Snapshots from the simulation of a bolaamphiphile forming a hexagonal columnar phase diluted with a benzene-like solvent, as a function of the concentration of the solvent. Reproduced with permission.[163] Copyright 2010, Royal Society of Chemistry.

We have already seen that simulations based on coarse grained molecular approach can lead to an understanding of the structure and dynamics in self-organised soft matter systems. There are, of course, other methods of coarse graining such systems. A fundamentally different approach is to use continuous fields rather than a molecule or particle-based approach. In this way, a many chain problem can be transformed into a number of single chain problems in the presence of an external (mean) field. These self-consistent field theory methods have been particularly useful for studies of polymer melts and blends. They work particularly well for diblock copolymer melts [165] in which the flexible polymer is well represented by a Gaussian chain. For more rigid molecules such as rod-coil polymers, this is not appropriate and the stiff section of the molecule requires a different treatment. [65,166,167] Although these methods have been used successfully to describe the phase structures of molecules at large (polymeric) length scales, they have not been widely or routinely used for small multi-block molecules such as bolaamphiphiles. Finally, in order to predict 3D and 2D morphologies of miktoarm star terpolymers (see Section 7), He and Liang[20a,b] have used dynamic density functional

theory[168] with considerable success. Furthermore, they extended their study to mixtures of ABC star polymers with one of the linear homopolymer components (A, B or C).[20c]

9 Outlook and potential applications

Attempts were made to use the polygonal honeycomb type LC phases to organize nanoparticles into ordered arrays. The effects of hydrophobic and hydrophilic nanoparticles on the mesophase stability of polygonal cylinder phases was investigated for compounds **1a** (n = 9, see Figure 1) and it was found that the columnar phase of this compound is gradually destabilised by an increasing concentration of hydrophobic alkyl-coated gold nano-clusters and gradually stabilized by increasing concentration of hydrophilic EO functionalized gold nanoparticles, but the mesophase structure itself does not seem to be changed significantly.[169] 3D ordered arrays of nanoparticles with rhombohedral symmetry were recently obtained with spherical gold nanoparticles to which rod-like molecules had been attached laterally.[170] In some respect these modified spherical nanoparticles also comprise some degree of polyphilicity as there is a degree of incompatibility between the aromatic rods, the spherical Au nanoparticles, the spacers and the terminal chains. Increasing the incompatibility could lead to additional options for new segregation-driven nanoparticle self assembly. This is of special interest for functional nanoparticles, as for example, magnetic [171] and semiconductor nanoparticles.[172]

Beside the organization of nanoparticles inside an ordered LC matrix, the nanoparticles themselves could also be functionalized so as to make them capable of soft self-assembly in a predefined way. Thus rod-like nanoparticles with tethered flexible chains could be used as rod-like building block. As suggested by recent simulation results such particles could indeed be able to self assemble into distinct superstructures,[173,174] among them polygonal honeycombs as observed for the X- and T-shaped polyphiles considered here. Hence, investigation of the molecular designing principles leading to different nano-scale LC morphologies with the molecules discussed herein could provide blueprints for appropriate functionalisation of nanoparticles for their self assembly in ordered arrays with defined geometries.

T- and X-shaped amphiphiles usually comprise elongated π-conjugated aromatics (oligothiophenes,[36] oligo(phenylene ethinylenes) [55,175]) which are of interest for application as fluorescent, luminescent[176] and semiconducting organic materials,[177] capable of self assembly into well defined superstructures. They can organize into bulk phases, into aqueous

lyotropic LC phases,[178] or into fibers and ribbons in a range of other solvents as demonstrated for rod-coil molecules with hydrophilic lateral groups[179] (Section 4). Alternatively they can self-assemble on surfaces, as illustrated in section 6.3). [103,104] Hence, the self assembly power of T-shaped and X-shaped polyphiles can be used for the alignment of π-conjugated aromatic systems in different defined ways for application in photoconductors, thin film transistors and photovoltaic devices. For example, oligo(phenylene vinylene) based facial amphiphiles, such as compound **15a** were used to obtain highly anisotropic films (order parameter 0.93) by spin-coating onto rubbed polymer alignment layers. In these layers the long axis of the rod-like cores is parallel to the surface, but the individual benzene rings adopt an edge-on orientation perpendicular to the surface.[180] The alignment was achieved without any further treatment and thus can be used for thin film electronic devices, a fact demonstrated by fabrication of a photovoltaic device. Dyads of the OPV compound **15b** with a lateral fullerene group lead to highly efficient dyad based solar cells.[181]

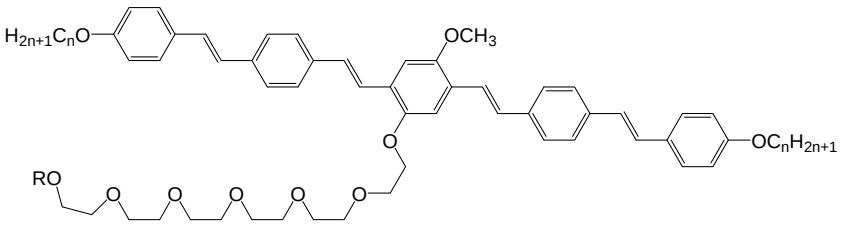

15a: R = H (*n* = 12)
15b: R = Fullerene containing unit (*n* = 1)

The cylinder structures of the T-and X-shaped amphiphiles themselves do not have hollow channels as they need to be filled by an appropriate volume of lateral chains. However, post self assembly fixation of the honeycombs once formed could provide permeable pores which could be used for selective transport of nonpolar (by using lateral substituted bolaamphiphiles) or polar guests (in the case of facial amphiphiles).

Besides self assembly, lithographic techniques could also be used to produce nanoscale patterns as required, for example, for integrated circuits. One of the main limitations is the difficulty in scaling the photolithographic techniques to smaller length scales below 100 nm. This requires strategies for producing a wide range of nanoscale patterns, especially square arrays that are compatible with technical standards. One promising technique to achieve this scaling is block copolymer (BCP) lithography, which affords feature sizes on a 10 to 100 nm

scale.[182] Square lattices were achieved at different length scales with star polymers (10-100 nm) and with T-shaped and X-shaped low molecular mass polyphiles at even smaller length scales between 3-10 nm. Hence, liquid crystals could provide materials for the next generation soft lithography, enabling a further step in pattern miniaturization.

Acknowledgements

The main support for the work covered by this review came from DFG and EPSRC with networking and management provided by the ESF Eurocores programme SONS2 through the collaborative project Complexity Across Length-Scales in Soft Matter (SCALES). The research and/or the preparation of the review was also supported by the European Union within European Regional Development Fund, through grant Innovative Economy (POIG.01.01.02-00-008/08) and by WCU program through the National Research Foundation of Korea funded by the Ministry of Education, Science and Technology (R31-10013).

References

[1] a) S. Stepanow, N. Lin, J. V. Barth, K. Kern, *J. Phys. Chem. B* **2006**, *110*, 23472; b) S. De Feyter, F. De Schryver, in *Supermolecular Dye Chemistry, Vol. 258* (Ed.: F. Würthner), Springer Berlin/Heidelberg, **2005**, pp. 205; c) S. De Feyter, F. C. De Schryver, *J. Phys. Chem. B* **2005**, *109*, 4290; d) Y. Li, Z. Ma, K. Deng, S. Lei, Q. Zeng, X. Fan, S. De Feyter, W. Huang, C. Wang, *Chem. Eur. J.* **2009**, *15*, 5418; e) D. Kühne, F. Klappenberger, R. Decker, U. Schlickum, H. Brune, S. Klyatskaya, M. Ruben, J. V. Barth, *J. Am. Chem. Soc.* **2009**, *131*, 3881; f) C. Lin, Y. Liu, S. Rinker, H. Yan, *ChemPhysChem* **2006**, *7*, 1641.

[2] a) A. F. Wells, *Three-Dimensional Nets and Polyhedra*, Wiley, New York, **1977**; b) B. Grünbaum, G. C. Shephard, *Tilings and Patterns*, W.H. Freeman, New York, **1987**.

[3] A. P. Côté, A. I. Benin, N. W. Ockwig, M. O'Keeffe, A. J. Matzger, O. M. Yaghi, *Science* **2005**, *310*, 1166.

[4] a) G. Férey, *Chem. Soc. Rev.* **2008**, *37*, 191; b) D. Maspoch, D. Ruiz-Molina, J. Veciana, *Chem. Soc. Rev.* **2007**, *36*, 770.

[5] C. Tschierske, *Chem. Soc. Rev.* **2007**, *36*, 1930.

[6] a) Y. Matsushita, K. Hayashida, A. Takano, *Macromol. Rapid Commun.* **2010**, *31*, 1579; b) V. Abetz, A. Boschetti-de-Fierro, J. F. Gohy, in *Controlled and Living Polymerizations:From Mechanisms to Applications* (Eds.: A. H. E. Müller, K. Matyjaszewski), Wiley-VCH, Weinheim, Germany, **2009**, pp. 493.

[7] N. Hadjichristidis, H. Iatrou, M. Pitsikalis, S. Pispas, A. Avgeropoulos, *Prog. Polym. Sci.* **2005**, *30*, 725.

[8] a) F. Tournilhac, L. Bosio, J. F. Nicoud, J. Simon, *Chem. Phys. Lett.* **1988**, *145*, 482; b) S. Pensec, F.-G. Tournilhac, P. Bassoul, C. Durliat, *J. Phys. Chem. B* **1998**, *102,* 52.

[9] Calamitic polyphiles incorporating perfluorinated segments have been reported and reviewed previously: F. Guittard, E.T. de Givenchy, S. Geribaldi, A. Cambon, *J. Fluorine Chem.* **1999**, *100*, 85; F. Guittard, S. Geribaldi, *J. Fluorine Chem.* **2001**, *107*, 363; X.-H. Liu, I. Manners, D.W. Bruce, *J. Mater. Chem.* **1998**, *8*, 1555; S.V. Arehart, C. Pugh, *J. Am. Chem. Soc.* **1997**, *119*, 3027; C. Pugh, J.-Y. Bae, J. Dharia, J.J. Ge,

S.Z.D. Cheng, *Macromolecules* **1998**, *31*, 5188; A.C. Small, D.K. Hunt, C. Pugh, *Liq. Cryst.* **1999,** *26*, 849.

[10] Examples of rod-like molecules incorporating oligo(siloxane) units: a) S. Diele, S. Oelsner, F. Kuschel, B. Hisgen, H. Ringsdorf, R. Zentel, *Makromol. Chem.***1987**, *188*, 1993; b) C. Pugh, J.-Y. Bae, J. Dharia, J. J. Ge, S. Z. D. Cheng, *Macromolecules* **1998**, *31*, 5188; c) W. K. Robinson, C. Carboni, P. Kloess, S. P. Perkins, H. J. Coles, *Liq. Cryst.* **1998***, 25*, 301; d) H. J. Coles, S. Meyer, P. Lehmann, R. Deschenaux, I. Jauslin, *J. Mater. Chem.* **1999**, *9*, 1085; e) G. H. Mehl, J. W. Goodby, *Chem. Commun*. **1999**, 13; f) D. Guillon, M. A. Osipov, S. Mery, M. Siffert, J.-F. Nicoud, C. Bourgogne, P. Sebastiao, *J. Mater. Chem.* **2001**, *11*, 2700; g) J. Naciri, D. K. Shenoy, P. Keller, S. Gray, K. Crandall, R. Shashidhar, *Chem. Mater.* **2002**, *14,* 5134; h) E. Nishikawa, E. T. Samulski, *Liq. Cryst*. **2000**, *27*, 1463; i) A. Komp, H. Finkelmann, *Macromol. Rapid Commun*. **2007**, *28*, 55.

[11] Silylated and fluorinated polycatenar molecules: a) M. F. Achard, M. F.; N.H. Tinh, H. Richard, M. Mauzac, F. Hardouin, *Liq. Cryst.* **1990**, *84*, 533; b) V. Percec, J. Heck, G. Ungar, *Macromolecules* **1991**, *24*, 4957; c) D. Lose, S. Diele, G. Pelzl, E. Dietzmann, W. Weissflog, *Liq. Cryst*. **1998**, *24*, 707; E. Nishikawa, J. Yamamoto, H. Yokoyama, *J. Mater. Chem*. **2003**, *13*, 1887. M. Gharbiaa, A. Gharbia, H.T. Nguyen, J. Malthete, *Curr. Opin. Colloid Interf. Sci*. **2002**, *7*, 312.

[12] Cyclosiloxanes: T. E. Mann, J. Haley, D. Lacey, *J. Mater. Chem.* **1999**, *9*, 353; L.-M. Liu, B.-Y. Zhang, X.-Z. He, C.-S. Cheng, *Liq. Cryst.* **2004**, *31*, 781.

[13] Polyphilic rod-like molecules incorporating hydrogenated and fluorinated alkyl chains or oligo(siloxane) segments (or combining both) became recently of interest for de Vries type smectic phases: a) J. P. F. Lagerwall, F. Giesselmann, *ChemPhysChem* **2006**, *7*, 20; b) M. Rössler, R. Zentel, J.P.F. Lagerwall, F. Giesselmann, *Liq. Cryst.* **2004**, *31*, 883; c) N. Olsson, B. Helgee, G. Andersson, L. Komitov, *Liq. Cryst.* **2005**, *32*, 1139; d) L. Li, C. D. Jones, J. Magolan, R. P. Lemieux, *J. Mater. Chem.* **2007**, *17*, 2313; J. C. Roberts, N. Kapernaum, F. Giesselmann, R. P. Lemieux, *J. Am. Chem. Soc.* **2008**, *130*, 13842.

[14] The concept of polyphilicity was recently also applied to bent-core molecules where the two distinct terminal chains were modified by adding fluorinated segments, oligo(siloxane) units or polar groups: a) R. A. Reddy, C. Tschierske, *J. Mater. Chem*. **2006**, *16*, 907; b) C. Keith, R.A. Reddy, A. Hauser, U. Baumeister, C. Tschierske, *J. Am. Chem. Soc***. 2006**, *126*, 3051; c) R. A. Reddy, U. Baumeister, C. Keith, H. Hahn, H. Lang, C. Tschierske, *Soft Matter* **2007**, *3*, 558; d) R.A. Reddy, G. Dantlgraber, U. Baumeister, C. Tschierske, *Angew. Chem. Int. Ed.* **2006**, *45*, 1928; D. Kardas, M. Prehm, U. Baumeister, D. Pociecha, R. A. Reddy, G. H. Mehl, C. Tschierske, *J. Mater. Chem.* **2005**, *15***,** 1722.

[15] Taper shaped molecules with fluorinated segments: V. Percec, G. Johansson, G. Ungar, J. Zhou, *J. Am. Chem. Soc.* **1996**, *118*, 9855; G. Johansson, V. Percec, G. Ungarn, J.P. Zhou, *Macromolecule,* **1996**, *29*, 646; G. Johansson, V. Percec, G. Ungarn, K. Smith, *Chem. Mater*. **1997**, *9*, 164.

[16] Metallomesogens with perfluorinated segments and polyphilic metallomesogens: M.-A. Guillevic, D.W. Bruce, *Liq. Cryst.* **2000,** *27,* 153; M.-A. Guillevic, T. Gelbrich, M.B. Hursthouse, D.W. Bruce, *Mol. Cryst. Liq. Cryst.* **2001**, *362,* 147; J. Szydlowska, A. Krowczynski, U. Pietrasik, A. Rogowska, *Liq. Cryst.* **2005**, *32,* 651; R. Dembinski, P. Spinet, S. Lentijo, M. W. Markowicz, J. M. Martin-Alvarez, A. L. Rheingold, D. J. Schmidt, A. Sniady, *Eur. J. Inorg. Chem*. **2008**, *10*, 1565; A. G1ebowska, P. Przybylski, M. Winek, P. Krzyczkowska, A. Krowczynski, J. Szyd1owska, D. Pociecha, E. Gorecka; *J. Mater. Chem*. **2009**, *19*, 1395; B. Bilgin-Eran, C. Tschierske,

S. Diele, U. Baumeister, *J. Mater. Chem*. **2006**, *16*, 1136; B. Bilgin-Eran, C. Tschierske, S. Diele, U. Baumeister, *J. Mater. Chem*. **2006**, *16*, 1145.
[17] J. Prost, R. Bruinsma, F. Tournilhac, *J. Phys. (Paris) II* **1994**, *4*, 169; S. S. Keast, M. E. Neubert, R. G. Petschek, *Liq. Cryst.* 1996, *21*, 695.
[18] S. I. Stupp, V. LeBonheur, K. Walker, L. S. Li, K. E. Huggins, M. Keser, A. Amstutz, *Science* **1997**, *276*, 384.
[19] U. Krappe, R. Stadler, I. Voigt-Martin, *Macromolecules*, **1995**, *28*, 4558.
[20] (a) X. H. He, H. J. Liang, C. Y. Pan, *J. Chem. Phys*. **2002**, *116*, 10508; (b) X. H. He, H. J. Liang, C. Y. Pan, *J. Chem. Phys*. **2003**, *118*, 9861; (c) T. Lu, X. H. He, H. J. Liang, *J. Chem. Phys*. **2004**, *121*, 9702.
[21] *Handbook of Liquid Crystals*, ed. D. Demus, J. Goodby, G. W. Gray, H.-W. Spiess, V. Vill, Wiley- VCH: Weinheim, **1998.**
[22] M. Kölbel, T. Beyersdorff, X. H. Cheng, C. Tschierske, J. Kain, S. Diele, *J. Am. Chem. Soc.* **2001**, *123*, 6809.
[23] a) X. Cheng, M. Prehm, M. K. Das, J. Kain, U. Baumeister, S. Diele, D. Leine, A. Blume, C. Tschierske, *J. Am. Chem. Soc.* **2003**, *125*, 10977; b) X. Cheng, M. K. Das, U. Baumeister, S. Diele, C. Tschierske, *J. Am. Chem. Soc.* **2004**, *126*, 12930.
[24] B. Chen, X. Zeng, U. Baumeister, G. Ungar, C. Tschierske, *Science* **2005**, *307*, 96.
[25] a) X. H. Cheng, M. K. Das, S. Diele, C. Tschierske, *Angew. Chem., Int. Ed.* **2002**, *41*, 4031; b) M. Prehm, X. H. Cheng, S. Diele, M. K. Das, C. Tschierske, *J. Am. Chem. Soc.* **2002**, *124*, 12072; c) M. Prehm, S. Diele, M. K. Das, C. Tschierske, *J. Am. Chem. Soc.* **2003**, *125*, 614; d) N. M. Patel, M. R. Dodge, M. H. Zhu, R. G. Petschek, C. Rosenblatt, M. Prehm, C. Tschierske, *Phys. Rev. Lett.* **2004**, *92*, 015501; e) N. M. Patel, C. Rosenblatt, M. Prehm, C. Tschierske, *Liq. Cryst.* **2005**, *32*, 55.
[26] A. Takano, W. Kawashima, A. Noro, Y. Isono, N. Tanaka, T. Dotera, Y. Matsushita, *J. Polymer Sci. B: Polymer Phys.* **2005**, *43*, 2427.
[27] B. Chen, U. Baumeister, S. Diele, M. K. Das, X. Zeng, G. Ungar, C. Tschierske, *J. Am. Chem. Soc.* **2004**, *126*, 8608.
[28] A. G. Cook, U. Baumeister, C. Tschierske, *J. Mater. Chem.* **2005**, *15*, 1708.
[29] B. Chen, U. Baumeister, G. Pelzl, M. K. Das, X. Zeng, G. Ungar, C. Tschierske, *J. Am. Chem. Soc.* **2005**, *127*, 16578.
[30] M. C. Holmes, *Curr. Opin. Colloid Interface Sci.* **1998**, *3*, 485.
[31] B. Chen, X. B. Zeng, U. Baumeister, S. Diele, G. Ungar, C. Tschierske, *Angew. Chem., Int. Ed.* **2004**, *43*, 4621.
[32] F. Liu, B. Chen, U. Baumeister, X. Zeng, G. Ungar, C. Tschierske, *J. Am. Chem. Soc.* **2007**, *129*, 9578.
[33] F. Liu, B. Chen, B. Glettner, M. Prehm, M. K. Das, U. Baumeister, X. Zeng, G. Ungar, C. Tschierske, *J. Am. Chem. Soc.* **2008**, *130*, 9666.
[34] X. Cheng, X. Dong, G. Wei, M. Prehm, C. Tschierske, *Angew. Chem., Int. Ed.* **2009**, *48*, 8014.
[35] X. Cheng, X. Dong, R. Huang, X. Zeng, G. Ungar, M. Prehm, C. Tschierske, *Chem. Mater.* **2008**, *20*, 4729.
[36] M. Prehm, G. Götz, P. Bäuerle, F. Liu, X. Zeng, G. Ungar, C. Tschierske, *Angew. Chem., Int. Ed.* **2007**, *46*, 7856.
[37] A. Mishra, C.-Q. Ma, and P. Bäuerle *Chem. Rev.* **2009,** *109,* 1141–1276.
[38] U. H. F. Bunz, *Macromol. Rapid Commun.* **2009**, *30*, 772.
[39] A. Mishra, C.-Q. Ma, P. Bäuerle *Chem. Rev.* **2009,** *109,* 1141–1276.
[40] a) Y.-J. Cheng, S.-H. Yang, C.-S. Hsu, *Chem. Rev.* **2009**, *109*, 5868; b) A. W. Hains, Z. Liang, M. A. Woodhouse, B. A. Gregg, *Chem. Rev.* **2010**, *110*, 6689; c) A. P. H. J. Schenning, E. W. Meijer, *Chem. Commun.* **2005**, 3245.

[41] B. Glettner, F. Liu, X. Zeng, M. Prehm, U. Baumeister, G. Ungar, C. Tschierske, *Angew. Chem., Int. Ed.* **2008**, *47*, 6080.
[42] R. A. Reddy, C. Tschierske *J. Mater. Chem*. **2006**, *16*, 907.
[43] G. Hennrich, A. Omenat, I. Asselberghs, S. Foerier, K. Clays, T. Verbiest, J. L. Serrano, *Angew. Chem., Int. Ed.* **2006**, *45*, 4203.
[44] M. Prehm, F. Liu, U. Baumeister, X. Zeng, G. Ungar, C. Tschierske, *Angew. Chem. Int. Ed.* **2007**, *46*, 7972.
[45] R. Kieffer, M. Prehm, K. Pelz, U. Baumeister, F. Liu, H. Hahn, H. Lang, G. Ungar, C. Tschierske, *Soft Matter* **2009**, *5*, 1214.
[46] M. Prehm, C. Enders, Maryam Y. Anzahaee, B. Glettner, U. Baumeister, C. Tschierske, *Chem. Eur. J.* **2008**, *14*, 6352.
[47] M. Prehm, F. Liu, X. Zeng, G. Ungar, C. Tschierske, *J. Am. Chem. Soc.* **2008**, *130*, 14922.
[48] R. Kieffer, M. Prehm, B. Glettner, K. Pelz, U. Baumeister, F. Liu, X. Zeng, G. Ungar, C. Tschierske, *Chem. Commun.* **2008**, 3861.
[49] G. Ungar, F. Liu, X. B. Zeng, B. Glettner, M. Prehm, R. Kieffer, C. Tschierske, *J. Phys., Conf. Series* **2010**, *247,* 012032.
[50] M. Prehm, G. Ungar, C. Tschierske, X.-B. Zeng, Unpublished results.
[51] S. Hassan, W. Rowe, G. J. T. Tiddy, in *Handbook of Applied Surface and Colloid Chemistry, Vol. 1* (Ed.: K. Holmberg), Wiley-VCH, Chichester, **2002**, p. 465.
[52] a) M. Gharbia, A. Gharbi, H. T. Nguyen, J. Malthete, *Curr. Opin. Colloid Interface Sci.* **2002**, *7*, 312; b) D. W. Bruce, *Acc. Chem. Res.* **2000**, *33*, 831.
[53] For a review of 3D structures in LC see G. Ungar, X. B. Zeng, *Soft Matter* **2005**, *1*, 95.
[54] B. M. Rosen, C. J. Wilson, D. A. Wilson, M. Peterca, M. R. Imam, V. Percec, *Chem. Rev.* **2009**, *109*, 6275.
[55] B. Glettner, F. Liu, X. Zeng, M. Prehm, U. Baumeister, M. Walker, Martin A. Bates, P. Boesecke, G. Ungar, C. Tschierske, *Angew. Chem., Int. Ed.* **2008**, *47*, 9063.
[56] Janus-molecules, named after the double-faced Roman god, are molecules with two sides of different chemistry or polarity: a) A. Walther, A. H. E. Müller, *Soft Matter* **2008**, *4*, 663; b) V. Percec, D. A. Wilson, P. Leowanawat, C. J. Wilson, A. D. Hughes, M. S. Kaucher, D. A. Hammer, D. H. Levine, A. J. Kim, F. S. Bates, K. P. Davis, T. P. Lodge, M. L. Klein, R. H. DeVane, E. Aqad, B. M. Rosen, A. O. Argintaru, M. J. Sienkowska, K. Rissanen, S. Nummelin, J. Ropponen, *Science* **2010**, *328*, 1009.
[57] X. B. Zeng, R. Kieffer, B. Glettner, C. Nürnberger, F. Liu, K. Pelz, M. Prehm, U. Baumeister, H. Hahn, H. Lang, G. A. Gehring, C. H. M. Weber, J. K. Hobbs, C. Tschierske, G. Ungar, *Science*, DOI: 10.1126/science. 1193052, accepted.
[58] M. Lee, B. K. Cho, W. C. Zin, *Chem. Rev.* **2001**, *101*, 3869; H. A. Klok, S. Lecommandoux, *Adv. Mater.* **2001**, *13*, 1217.
[59] B. D. Olsen, R. A. Segalman, *Mater. Sci. Eng*. **2008**. *R62*, 37.
[60] C.L. Chochos, J.K. Kallitsis, V.G. Gregoriou, *J. Phys. Chem. B* **2005**, *109*, 8755; S. Becker, C. Ego, A.C. Grimsdale, E.J.W. List, D. Marsitzky, A. Pogantsch, S. Setayesh, G. Leising, K. Müllen, *Synth. Metals* **2001**, *125*, 73; G. Yu, J. Gao, J.C. Hummelen, F. Wudl, A.J. Heeger, *Science* **1995**, *270*, 1789.
[61] U. Stalmach, B. de Boer, A.D. Post, P.F. van Hutten, G. Hadziioannou, *Angew. Chem. Int. Ed.* **2001**, *40*, 428; K. van de Wetering, C. Brochon, C. Ngov, G. Hadziioannou, *Macromolecules* **2006**, *39*, 4289; J.A. Osaheni, S.A. Jenekhe, *J. Am. Chem. Soc*. **1995**, *117*, 7389;
[62] H.A. Klok, J.F. Langenwalter, S. Lecommandoux, *Macromolecules* **2000**, *33*, 7819.
[63] M.W. Neiser, S. Muth, U. Kolb, J.R. Harris, J. Okuda, M. Schmidt, *Angew. Chem. Int. Ed.* **2004**, *43*, 3192; C.X. Cheng, Y. Tian, Y.Q. Shi, R.P. Tang, F. Xi, *Langmuir* **2005**,

21, 6576; Y. Yi, X.H. Wan, X.H. Fan, R. Dong, Q.F. Zhou, *J. Polym. Sci. Pt. A - Polym. Chem.* **2003**, *41*, 1799.
[64] R. Holyst, M. Schick, *J. Chem. Phys.* **1992**, *96*, 730.
[65] Y. Xia, Z. Sun, T. Shi, J. Chen, L. An, Y. Jia *Polymer* **2008**, *49*, 5596.
[66] N. Sary, L. Rubatat, C. Brochon, G. Hadziioannou, J. Ruokolainen, R. Mezzenga, *Macromolecules* **2007**, *40*, 6990.
[67] J. T. Chen, E. L. Thomas, C. K. Ober, S. S. Hwang *Macromolecules* **1995**, *28*, 1688; J. T. Chen, E. L. Thomas, C. K. Ober, S. S. Hwang, *Science* **1997**, *273*, 343; N. K. Oh, W. C. Zin, J. Hwan, M. Lee *Polymer* **2006**, *47*, 5275.
[68] S.A. Jenekhe, X.L. Chen, *J. Phys. Chem. B* **2000**, *104*, 6332.
[69] D.-J. Hong, E. Lee, J.-K. Lee, W.-C. Zin, M. Han, E. Sim, M. Lee, *J. Am. Chem. Soc.* **2008**, *130*, 14448.
[70] a) E. Lee, J.-K. Kim, M. Lee, *Angew. Chem. Int. Ed*. **2009**, *48*, 3657-3660 b) D. J. Hong, E. Lee, H. Jeong, J. k. Lee, W. C. Zin, T. Nguyen, S. Glotzer, M. Lee, *Angew. Chem. Int. Ed.* **2009**, *48*, 1664.
[71] E. Lee, J.-K. Kim, M. Lee, *J. Am. Chem. Soc.* **2009**, *131*, 18242.
[72] H.-J. Kim, Y.-H. Jeong, E. Lee, M. Lee, *J. Am. Chem. Soc.* **2009**, *131*, 17371.
[73] The actual molecular conformation in the self assembled mesophases can be different from Y-shaped.[74]
[74] a) M. Lehmann, M. Jahr, J. Gutmann, *J. Mater. Chem*. **2008**, *18*, 2995; b) M. Lehmann, *Chem. Eur. J*. **2009**, *15*, 3638.
[75] D. Davidson, A. M. Levelut, H. Strzelecka, V. Gionis, *J. Phys. Lett.* **1983**, *44*, L-823; S. Mery, D. Haristoy, J.-F. Nicoud, D. Guillon, S. Diele, H. Monobe, Y. Shimizu, *J. Mater. Chem*. **2002**, *12*, 37;
[76] P. H. J. Kouwer, S. J. Picken, G. H. Mehl, *J. Mater. Chem*. **2007**, *17*, 4196.
[77] a) A. Kohlmeier, D. Janietz, *Liq. Cryst*. **2007**, *34*, 289; b) D. Janietz, A. Kohlmeier, *Mol. Cryst. Liq. Cryst.*,**2009**, *509*, 39; c) D. Janietz, A. Kohlmeier, *Liq. Cryst*. **2009**, *36*, 685.
[78] V. Percec, M. R. Imam, T. K. Bera, V. S. K. Balagurusamy, M. Peterca, P. A. Heiney *Angew. Chem. Int. Ed*. **2005**, *44*, 4739.
[79] X. Cheng, X. Bai, S. Jing, H. Ebert, M. Prehm, C. Tschierske, *Chem. Eur. J*. **2010**, *16*, 4588.
[80] Y. Hendrikx, A. M. Levelut. *Mol. Cryst. Liqu. Cryst*. **1988**, *165*, 233.
[81] M. Peterca, M. R. Imam, P. Leowanawat, B. M. Rosen, D. A. Wilson, C. J. Wilson, X. B. Zeng, G. Ungar, P. A. Heiney, V. Percec, *J. Am. Chem. Soc*. **2010**, *132*, 11288.
[82] M. A. Shcherbina, X.Zeng, T. Tadjiev, G.Ungar, S.H.Eichhorn, K. E. S.Phillips, T.J. Katz, *Angew. Chem. Int. Ed.* **2009**, *48*, 7837.
[83] J. W. Goodby, I. M. Saez, S. J. Cowling, V. Görtz, M. Draper, A. W. Hall, S. Sia, G. Cosquer, S.-E. Lee, E. P. Raynes, *Angew. Chem. Int. Ed*. **2008**, *47*, 2754; I. M. Saez, J. W. Goodby, *J. Mater. Chem*. **2005**, *15*, 26; I. M. Saez, J. W. Goodby, *Chem. Eur. J.* **2003**, *9*, 4869; I. M. Saez, J. W. Goodby, *J. Mater. Chem*., **2003**, *13*, 2727.
[84] A. Yamaguchi, N. Uehara, J. Yamamoto, A. Yoshizawa, *Chem. Mater.* **2007,** *19,* 6445.
[85] a) I. Bury, B. Heinrich, C. Bourgogne, D. Guillon, B. Donnio *Chem. Eur. J*. **2006**, *12*, 8396; b) V. Percec, D. A. Wilson, P. Leowanawat, C. J. Wilson, A. D. Hughes, M. S. Kaucher, D. A. Hammer, D. H. Levine, A. J. Kim, F. S. Bates, K. P. Davis, T. P. Lodge, M. L. Klein, R. H. DeVane, E. Aqad, B. M. Rosen, A. O. Argintaru, M. J. Sienkowska, K. Rissanen, S. Nummelin, J. Ropponen, *Science* **2010**, *328*, 1009.
[86] S. Hernandez-Aisa, J. Barbera, M. Marcos, J. L. Serrano, *Chem. Mater*. **2010**, *22*, 4762.

[87] R. W. Date, D. W. Bruce *J. Am. Chem. Soc.* **2003**, *125*, 9012; P. H. J. Kouwer, G. H. Mehl, *J. Mater. Chem*., **2009**, *19*, 1564.
[88] a) V. Percec, M. Glodde, M. Peterca, A. Rapp, I. Schnell, H. W. Spiess, T. K. Bera, Y. Miura, V. S. K. Balagurusamy, E. Aqad and P. A. Heiney, *Chem. Eur. J*., **2006**, *12*, 6298; b) A. Schaz, G. Lattermann, *Liq. Cryst.* **2005**, *32*, 407; c) A. Schaz, E. Valaityte, G. Lattermann, *Liq. Cryst.* **2005**, *32*, 513; d) B. Bilgin-Eran, C. Yorur, C. Tschierske, M. Prehm, U. Baumeister, *J. Mater. Chem*., 2007, *17*, 2319.
[89] A. Zelcer, B. Donnio, C. Bourgogne, F. D. Cukiernik, D. Guillon, *Chem. Mater.* **2007**, *19*, 1992.
[90] L. Cui, J. Miao, L. Zhu, *Macromolecules* **2006,** *39,* 2536; S. Sauer, N. Steinke, A. Baro, S. Laschat, F. Giesselmann, W. Kantlehner, *Chem. Mater.* **2008**, *20,* 1909; I. Paraschiv, M. Giesbers, B. van Lagen, F. C. Grozema, R. D. Abellon, L. D. A. Siebbeles, A. T. M. Marcelis, H. Zuilhof, E. J. R. Sudhölter, *Chem. Mater.* **2006,** *18,* 968; C. F. C. Fitié, I. Tomatsu, D. Byelov, W. H. de Jeu, R. P. Sijbesma, *Chem. Mater.* **2008**, *20,* 2394; S. Kumar, S. Kumar Pal, *Tetrahedron Lett*. **2005**, *46*, 2607; J. Motoyanagi, T. Fukushima, T. Aida, *Chem. Commun*. **2005**, 101; M. Akhtarul Alam, J. Motoyanagi, Y. Yamamoto, T. Fukushima, J. Kim, K. Kato, M. Takata, A. Saeki, S. Seki, S. Tagawa, T. Aida, *J. Am. Chem. Soc*. **2009**, *131*, 17722.
[91] D. W. Berreman, *Phys. Rev. Lett.* **1972**, *28*, 1683.
[92] M. Schadt, K. Schmitt, V. Kozinkov, V. Chigrinov, *Jpn. J. Appl. Phys.* **1992**, *31*, 2155.
[93] T. Uchida, H. Seki, in *Liquid Crystals: Applications and Uses* (Ed.: B. Bahadur), World Scientific, Singapore **1992**.
[94] Y. H. Kim, D K. Yoon H.-T. Jung, *J. Mater. Chem.* **2009**, *19*, 9091.
[95] a) E. Grelet, H. Bock, *Europhys. Lett.* **2006**, *73*, 712; b) E. Grelet, S. Dardel, H. Bock, M. Goldmann, E. Lacaze, F. Nallet, *Eur. Phys. J. E* **2010**, *31*, 343.
[96] a) T. S. Perova, J. K. Vij, A. Kocot, *Europhys. Lett.* **1998**, *44*, 198; b) S. H. Eichhorn, A. Adavelli, H. S. Li, N. Fox, *Mol. Cryst. Liq. Cryst.* **2003**, *397*, 47.
[97] V. Percec, G. Johansson, G. Ungar, J. Zhou, *J. Am. Chem. Soc.* **1996**, *118*, 9855.
[98] J. P. Bramble, D. J. Tate, D. J. Revill, K. H. Sheikh, J. R. Henderson, F. Liu, X. Zeng, G. Ungar, R. J. Bushby, S. D. Evans, *Adv. Funct. Mater.* **2010**, *20*, 914.
[99] X. Zeng, M. Prehm, R. Zhang, F. Liu, S. Grimm, M. Geuss, M. Steinhart, C. Tschierske, G. Ungar, submitted.
[100] A. Ulman, *An Introduction to Ultrathin Organic Films: From Langmuir-Blodgett to Self-assembly*, Academic Press, Boston, **1991**.
[101] Q. Zhou, T. Chen, J. Zhang, L. Wan, P. Xie, C. C. Han, S. Yan, R. Zhang, *Tetrahedron Lett.* **2008**, *49*, 5522.
[102] G. L. Gaines, *Insoluble monolayers at Liquid-Gas Interfeces*, Interscience, New York, **1966**.
[103] a) J. A. Schröter, R. Plehnert, C. Tschierske, S. Katholy, D. Janietz, F. Penacorada, L. Brehmer, *Langmuir* **1997**, *13*, 796; b) R. Plehnert, J. A. Schröter, C. Tschierske, *Langmuir* **1998**, *14*, 5245; c) R. Plehnert, J.-A. Schröter, C. Tschierske, *Langmuir* **1999**, *15*, 3773.
[104] P. Nitoń, A. Zywocinski, R. Holyst, R. Kieffer, C. Tschierske, J. Paczesny, D. Pociecha, E. Gorecka, *Chem. Commun.* **2010**, *46*, 1896.
[105] a) D. J. Tweet, R. Holstrokyst, B. D. Swanson, H. Stragier, L. B. Sorensen, *Phys. Rev. Lett.* **1990**, *65*, 2157; b) R. Hołyst, *Phys. Rev. A* **1991**, *44*, 3692.
[106] a) M. Ibn-Elhaj, H. Möhwald, M. Z. Cherkaoui, R. Zniber, *Langmuir* **1998**, *14*, 504; b) M. Ibn-Elhaj, H. Riegler, ouml, H. hwald, M. Schwendler, C. A. Helm, *Phys. Rev. E* **1997**, *56*, 1844.

[107] M. N. G. de Mul, J. A. Mann, *Langmuir* **1994**, *10*, 2311.
[108] B. Rapp, H. Gruler, *Phys. Rev. A* **1990**, *42*, 2215.
[109] M. C. Friedenberg, G. G. Fuller, C. W. Frank, C. R. Robertson, *Langmuir* **1994**, *10*, 1251.
[110] M. Badis, M. H. Guermouche, J.-P. Bayle, M. Rogalski, E. Rogalska, *Langmuir* **2004**, *20*, 7991.
[111] F. G. Tournilhac, L. Bosio, J. P. Bourgoin, M. Vandevyver, *J. Phys. Chem.* **1994**, *98*, 4870.
[112] M. Pérez-Morales, J. M. Pedrosa, M. T. Martín-Romero, D. Möbius, L. Camacho, *J. Phys. Chem. B* **2004**, *108*, 4457.
[113] N. Mizoshita, T. Seki, *Soft Matter* **2006**, *2*, 157.
[114] J. J. Haycraft, C. A. DeVries, H. Garcia Flores, A. Lech, J. P. Hagen, C. J. Eckhardt, *Thin Solid Films* **2007**, *515*, 2990.
[115] A. M. González-Delgado, M. Pérez-Morales, J. J. Giner-Casares, E. Muñoz, M. a. T. Martín-Romero, L. Camacho, *J. Phys. Chem. B* **2009**, *113*, 13249.
[116] a) L. Liu, J. K. Kim, M. Lee, *ChemPhysChem* **2010**, *11*, 706; b) L. Liu, D.-J. Hong, M. Lee, *Langmuir* **2009**, *25*, 5061.
[117] R.A. Segalman, *Mater. Sci. Eng. R* **2005**, *48*, 191.
[118] V. Abetz, A. Boschetti-de-Fierro, J. F. Gohy, in *Controlled and Living Polymerizations:From Mechanisms to Applications* (Eds.: A. H. E. Müller, K. Matyjaszewski), Wiley-VCH, Weinheim, Germany, **2009**, pp. 493.
[119] V. Abetz, P. F. W. Simon, *Adv. Polymer Sci.* **2005**, *189*, 125.
[120] R. Hosemann, S. N. Bagchi, *Direct Analysis of Diffraction by Matter,* North-Holland, Amsterdam, Netherlands,**1962**.
[121] T. Fujimoto, H. Zhang, T. Kazama, Y. Isono, H. Hasegawa, T. Hashimoto, *Polymer* **1992**, *33*, 2208.
[122] S. Okamoto, H. Hasegawa, T. Hashimoto, T. Fujimoto, H. Zhang, T. Kazama, A. Takano, Y. Isono, *Polymer* **1997**, *38*, 5275.
[123] S. Sioula, N. Hadjichristidis, E. L. Thomas, *Macromolecules* **1998**, *31*, 5272.
[124] S. Sioula, N. Hadjichristidis, E. L. Thomas, *Macromolecules* **1998**, *31*, 8429.
[125] Y. Matsushita, K. Yamada, T. Hattori, T. Fujimoto, Y. Sawada, M. Nagasawa, C. Matsui, *Macromolecules* **1983**, *16*, 10.
[126] K. Yamauchi, K. Takahashi, H. Hasegawa, H. Iatrou, N. Hadjichristidis, T. Kaneko, Y. Nishikawa, H. Jinnai, T. Matsui, H. Nishioka, M. Shimizu, H. Furukawa, *Macromolecules* **2003**, *36*, 6962.
[127] K. Yamauchi, S. Akasaka, H. Hasegawa, H. Iatrou, N. Hadjichristidis, *Macromolecules* **2005**, *38*, 8022.
[128] H. Hückstädt, V. Abetz, R. Stadler, *Macromol. Rapid Commun.* **1996**, *17*, 599.
[129] H. Hückstädt, A. Göpfert, V. Abetz, *Macromol. Chem. Phys.* **2000**, *201*, 296.
[130] H. Hückstädt, T. Goldacker, A. Göpfert, V. Abetz, *Macromolecules* **2000**, *33*, 3757.
[131] V. Abetz, in "Forschungsförderung 1998, Kurzberichte über Forschungsarbeiten, die aus Mitteln der Arbeitsgemeinschaft industrieller Forschungsvereinigungen e.V. (AIF) und der Max-Buchner-Forschungsstiftung gefördert worden sind" of DECHEMA e.V.
[132] A. Hirao, T. Higashihara, K. Inoue, *Macromolecules* **2008**, *41*, 3579.
[133] A. Gitsas, G. Floudas, M. Mondeshki, I. Lieberwirth, H. W. Spiess, H. Iatrou, N. Hadjichristidis, A. Hirao, *Macromolecules* **2010**, *43*, 1874.
[134] V. Abetz, in *Encyclopedia of Polymer Science and Technology*, Vol. 1 (Ed: J. I. Kroschwitz), John Wiley & Sons, Inc., **2003**, 482.
[135] V. Abetz, S. Jiang, *e-Polymers* **2004**, no.54.
[136] T. M. Birshtein, A. A. Polotsky, V. Abetz, *Macromol. Theory Simul.* **2004**, *13*, 512.

[137] A. Takano, S. Wada, S. Sato, T. Araki, K. Hirahara, T. Kazama, S. Kawahara, Y. Isono, A. Ohno, N. Tanaka, Y. Matsushita, *Macromolecules* **2004**, *37*, 9941.
[138] a) Y. Matsushita, *Polym. J.* **2008**, *40*, 177; b) Y. Matsushita, A. Takano, K. Hayashida, T. Asari, A. Noro, *Polymer* **2009**, *50*, 2191 and references therein.
[139] A. K. Sinha, *Topologically Close Packed Structures of TransitionMetal Alloys*, Pergamon Press, Oxford **1972**.
[140] A. Takano, W. Kawashima, A. Noro, Y. Isono, N. Tanaka, T. Dotera, Y. Matsushita, *J. Polymer Sci. B: Polymer Phys.* **2005**, *43*, 2427.
[141] a) X. B. Zeng, G. Ungar, Y. S. Liu, V. Percec, A. s. E. Dulcey, J. K. Hobbs, *Nature* **2004**, *428*, 157; b) X. Zeng, G. Ungar, *Phil. Mag.* **2006**, *86*, 1093.
[142] K. Hayashida, A. Takano, T. Dotera, Y. Matsushita, *Macromolecules* **2008**, *41*, 6269.
[143] a) K. Borisch, S. Diele, P. Goring, C. Tschierske, *Chem. Commun.* **1996**, 237; b) K K. Borisch, S. Diele, P. Göring, H. Müller, C. Tschierske, *Liq. Cryst.* **1997**, *22*, 427; c) K. Borisch, S. Diele, P. Göring, H. Kresse, C. Tschierske, *Angew. Chem. Int. Ed.* **1997**, *36*, 2087.
[144] a) V. S. K. Balagurusamy, G. Ungar, V. Percec, G. Johansson, *J. Am. Chem. Soc.* **1997**, *119*, 1539; b) S. D. Hudson, H.-T. Jung, V. Percec, W.-D. Cho, G. Johansson, G. Ungar, V. S. K. Balagurusamy, *Science* **1997**, *278*, 449; c) D. R. Dukeson, G. Ungar, V. S. K. Balagurusamy, V. Percec, G. A. Johansson, M. Glodde, *J. Am. Chem. Soc.* **2003**, *125*, 15974.
[145] G. Ungar, Y. S. Liu, X. B. Zeng, V. Percec, W. D. Cho, *Science* **2003**, *299*, 1208.
[146] S. Junnila, N. Houbenov, S. Hanski, H. Iatrou, A. Hirao, N. Hadjichristidis,. O. Ikkala, *Macromolecules* **2010**, *43*, 9071.
[147] D. Frenkel, B. Smit, *Understanding Molecular Simulation: From Algorithms to Applications*, Academic Press, **2002**.
[148] J. G. Gay, B. J. Berne, *J. Chem. Phys.* **1981**, *74*, 3316.
[149] M. A. Bates, G. R. Luckhurst, *J. Chem. Phys.* **1999**, *110*, 7087.
[150] M. A. Bates, G. R. Luckhurst, *J. Chem. Phys.* **2004**, *120*, 394.
[151] M. A. Bates, G. R. Luckhurst, *Mol. Phys.* **2001**, *99*, 1365.
[152] M. A. Bates, G. R. Luckhurst, *J. Chem. Phys.* **2003**, *118*, 6605.
[153] M. A. Bates, *Liq. Cryst.* **2005**, *32*, 1365.
[154] J. Baschnagel, K. Binder, P. Doruker, A. A. Gusev, O. Hahn, K. Kremer, W. L. Mattice, F. Müller-Plathe, M. Murat, W. Paul, S. Santos, U. W. Suter, V. Tries, in *Adv. Polym. Sci.*, Vol. 152, **2000**, 41.
[155] K. Kremer, G. S. Grest, *J. Chem. Phys.* **1990**, *92*, 5057.
[156] a) P. J. Hoogerbrugge, J. M. V. A. Koelman, *Europhys. Lett.* **1992**, *19*, 155; b) J. M. V. A. Koelman, P. J. Hoogerbrugge, *Europhys. Lett.* **1993**, *21*, 363.
[157] a) R. D. Groot, P. B. Warren, *J. Chem. Phys.* **1997**, *107*, 4423; b) R. D. Groot, T. J. Madden, *J. Chem. Phys.* **1998**, *108*, 8713.
[158] A. AlSunaidi, W. K. d. Otter, J. H. R. Clarke, *J. Chem. Phys.* **2009**, *130*, 124910.
[159] a) J. Xin, D. Liu, C. Zhong, *J. Phys. Chem. B* **2007**, *111*, 13675; b) J. Xia, C. Zhong, *Macromol. Rapid Commun.* **2006**, *27*, 1110.
[160] M. Bates, M. Walker, *Soft Matter* **2009**, *5*, 346.
[161] M. A. Bates, M. Walker, *Phys. Chem. Chem. Phys.* **2009**, *11*, 1893.
[162] A. J. Crane, F. J. Martinez-Veracoechea, F. A. Escobedo, E. A. Müller, *Soft Matter* **2008**, *4*, 1820.
[163] A. J. Crane, E. A. Müller, *Faraday Discussions* **2010**, *144*, 187.
[164] M. A. Bates, M. Walker, *Mol. Cryst. Liq. Cryst.* **2010**, *525*, 204.
[165] M. W. Matsen, *Macromolecules*, **1995**, *28*, 2765.

[166] M. W. Matsen, C. Barrett, *J. Chem. Phys.* **1998**, *109*, 4108; V. Pryamisyn, V. Ganesan, *J. Chem. Phys*. **2004**,*120*, 5824.
[167] W.T. Li, D. Gersappe, *Macromolecules* **2001**, *34*, 6783.
[168] J. G. E. M. Fraaije, B. A. C. Van Vlimmeren, N. M. Maurits, M. Postma, O. A. Evers, C. Hoffmann, G. Goldbeck-Wood, *J. Chem. Phys*. **1997**, *106*, 4260.
[169] H. Qi, A. Lepp, P. A. Heiney, T. Hegmann, *J. Mater. Chem.* **2007**, *17*, 2139.
[170] X. Zeng, F. Liu, A. G. Fowler, G. Ungar, L. Cseh, G. H. Mehl, J. E. Macdonald, *Adv. Mater.* **2009**, *21*, 1746.
[171] a) E. Terazzi, C. Bourgogne, R. Welter, J. L. Gallani, D. Guillon, G. Rogez, B. Donnio, *Angew. Chem. Int. Ed.* **2008**, *47*, 490; b) B. Donnio, P. García-Vázquez, J.-L. Gallani, D. Guillon, E. Terazzi, *Adv. Mater.* **2007**, *19*, 3534.
[172] a) S. Meuer, K. Fischer, I. Mey, A. Janshoff, M. Schmidt, R. Zentel, *Macromolecules* **2008**, *41*, 7946; b) S. Meuer, P. Oberle, P. Theato, W. Tremel, R. Zentel, *Adv. Mater.* **2007**, *19*, 2073.
[173] L. He, L. Zhang, Y. Ye, H. Liang, *J. Phys. Chem. B* **2010**, *114*, 7189.
[174] a) T. D. Nguyen, S. C. Glotzer, *ACS Nano* **2010**, *4*, 2585; b) M. A. Horsch, Z. Zhang, S. C. Glotzer, *Soft Matter* **2010**, *6*, 945; c) T. D. Nguyen, Z. Zhang, S. C. Glotzer, *J Chem. Phys.* **2008**, *129*, 244903.
[175] a) U. H. F. Bunz, *Macromol. Rapid Commun.* **2009**, *30*, 772; b) L. Kloppenburg, D. Jones, J. B. Claridge, H.-C. zur Loye, U. H. F. Bunz, *Macromolecules* **1999**, *32*, 4460.
[176] R. Thomas, S. Varghese, G. U. Kulkarni, *J. Mater. Chem.* **2009**, *19*, 4401.
[177] a) W. Pisula, M. Zorn, J. Y. Chang, K. Müllen, R. Zentel, *Macromol. Rapid Commun.* **2009**, *30*, 1179; b) M. O'Neill, S. Kelly, *Adv. Mater.* **2003**, *15*, 1135; c) J. Wu, W. Pisula, K. Müllen, *Chem. Rev.* **2007**, *107*, 718; d) S. Sergeyev, W. Pisula, Y. H. Geerts, *Chem. Soc. Rev.* **2007**, *36*, 1902.
[178] J. A. Schröter, C. Tschierske, M. Wittenberg, J. H. Wendorff, *J. Am. Chem. Soc.* **1998**, *120*, 10669.
[179] E. Lee, Z. Huang, J. H. Ryu, M. Lee, *Chem. Eur. J.* **2008**, *14*, 6957.
[180] T. Nishizawa, H. K. Lim, K. Tajima, K. Hashimoto, *J. Am. Chem. Soc.* **2009**, *131*, 2464.
[181] T. Nishizawa, H. K. Lim, K. Tajima, K. Hashimoto, *Chem. Commun.* **2009**, 2469.
[182] a) V. P. Chuang, J. Gwyther, R. A. Mickiewicz, I. Manners, C. A. Ross, *Nano Lett.* **2009**, *9*, 4364; b) C. Tang, E. M. Lennon, G. H. Fredrickson, E. J. Kramer, C. J. Hawker, *Science* **2008**, *322*, 429.